USGS
science for a changing world

Prepared in cooperation with the Edwards Aquifer Authority

Geologic Framework and Hydrostratigraphy of the Edwards and Trinity Aquifers Within Northern Bexar and Comal Counties, Texas

Pamphlet to accompany

Scientific Investigations Map 3510

Supersedes USGS Scientific Investigations Map 3366

U.S. Department of the Interior
U.S. Geological Survey

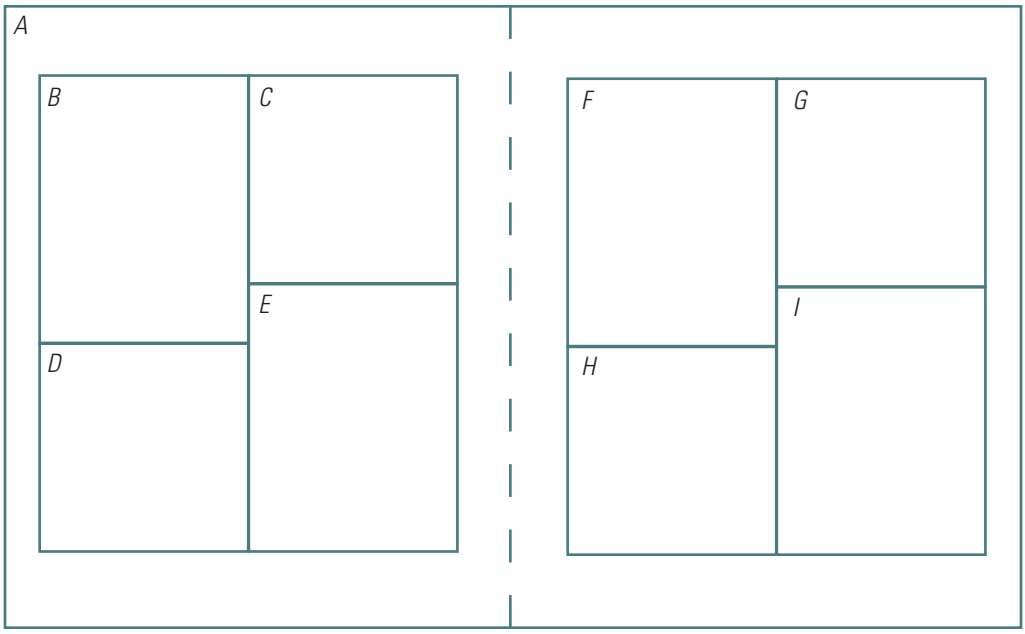

Front cover.

A, Photograph showing Cibolo Creek near Camp Bullis, Texas (lat 29°44′38″ N., long 98°37′24″ W.), with water flowing over the lower member of the Glen Rose Limestone of the Trinity Group (Herff Falls hydrostratigraphic unit of the middle zone of the Trinity aquifer). Photograph by Allan K. Clark, U.S. Geological Survey, May 31, 2007.

B, Photograph showing *Skolithos* burrows in hydrostratigraphic unit VII of the Edwards aquifer, dolomitic member of the Kainer Formation (lat 29°46′14″ N., long 98°16′12″ W.), south-central Texas. Photograph by Allan K. Clark, U.S. Geological Survey, August 5, 2014.

C, Photograph showing karst features developed along bedding plane porosity in the dolomitic member of the Edwards Group (hydrostratigraphic unit VII) west of Bella Loma Drive, San Antonio, Texas (lat 29°37′33″ N., long 98°37′14″ W.). Photograph by Allan K. Clark, U.S. Geological Survey, June 26, 2014.

D, Photograph showing dinosaur footprints in the upper member of the Glen Rose Limestone (cavernous hydrostratigraphic unit) west of Sattler, Texas (lat 29°50′16″ N., long 98°13′15″ W.). Photograph by Allan K. Clark, U.S. Geological Survey, December 1, 2015.

E, Photograph showing footwall of normal fault in the outcrop of the Edwards Group in northern Bexar County, Texas (lat 29°36′26″ N., long 98°34′57″ W.). Photograph by Allan K. Clark, U.S. Geological Survey, February 7, 2014.

Back cover.

F, Photograph showing Cibolo Creek in eastern Bexar County, Texas (lat 29°42′11″ N., long 98°22′50″ W.), with water flowing over the upper member of the Glen Rose Limestone of the Trinity Group (cavernous hydrostratigraphic unit of the upper zone of the Trinity aquifer). Photograph by Allan K. Clark, U.S. Geological Survey, August 9, 2014.

G, Photograph showing grainstone member of the Edwards Group (hydrostratigraphic member V of the Edwards aquifer) north of Helotes, Texas (lat 29°35′30″ N., long 98°44′12″ W.). Photograph by Allan K. Clark, U.S. Geological Survey, June 14, 2018.

H, Photograph showing geologic section in northern Bexar County (lat 29°39′27″ N., long 98°39′10″ W.). Photograph by Allan K. Clark, U.S. Geological Survey, August 1, 2014.

I, Photograph showing Allan K. Clark, U.S. Geological Survey, preparing to photograph the interior of Bear Cave to build a virtual tour of the cave. The cave is located in northern Bexar County, Texas (lat 29°38′51″ N., long 98°28′18″ W.). Photograph by Robert R. Morris, U.S. Geological Survey, June 15, 2023.

Geologic Framework and Hydrostratigraphy of the Edwards and Trinity Aquifers Within Northern Bexar and Comal Counties, Texas

By Allan K. Clark, James A. Golab, Robert R. Morris, and Diana E. Pedraza

Prepared in cooperation with the Edwards Aquifer Authority

Pamphlet to accompany
Scientific Investigations Map 3510
Supersedes USGS Scientific Investigations Map 3366

U.S. Department of the Interior
U.S. Geological Survey

U.S. Geological Survey, Reston, Virginia: 2023
Supersedes USGS Scientific Investigations Map 3366

Suggested citation:
Clark, A.K., Golab, J.A., Morris, R.R., and Pedraza, D.E., 2023, Geologic framework and hydrostratigraphy of the Edwards and Trinity aquifers within northern Bexar and Comal Counties, Texas: U.S. Geological Survey Scientific Investigations Map 3510, 1 sheet, scale 1:24,000, 24-p. pamphlet, https://doi.org/10.3133/sim3510. [Supersedes USGS Scientific Investigations Map 3366.]

Associated data for this publication:
Pedraza, D.E., Clark, A.K., Golab, J.A., and Morris, R.R., 2023, Geospatial dataset for the geologic framework and hydrostratigraphy of the Edwards and Trinity aquifers within northern Bexar and Comal Counties, Texas, at 1:24,000: U.S. Geological Survey data release, https://doi.org/10.5066/P9GXJ2RS.

ISSN 2329-132X (online)

Acknowledgments

The authors thank the landowners and managers of private and public lands in Bexar and Comal Counties, Texas, who provided access to their property for this study. We extend particular thanks to Ronald G. Fieseler, general manager of the Blanco-Pedernales Groundwater Conservation District, for helping to arrange access to private lands.

Contents

Sheet

[https://doi.org/10.3133/sim3510]

Geologic framework and hydrostratigraphy of the Edwards and Trinity aquifers within northern Bexar and Comal Counties, Texas

Figures

[On sheet]

Conversion Factors

U.S. customary units to International System of Units

Multiply	By	To obtain
	Length	
inch (in.)	2.54	centimeter (cm)
inch (in.)	25.4	millimeter (mm)
foot (ft)	0.3048	meter (m)
mile (mi)	1.609	kilometer (km)
	Area	
square mile (mi^2)	259.0	hectare (ha)
square mile (mi^2)	2.590	square kilometer (km^2)

International System of Units to U.S. customary units

Multiply	By	To obtain
	Length	
meter (m)	3.281	foot (ft)
kilometer (km)	0.6214	mile (mi)

Datum

Vertical coordinate information is referenced to the North American Vertical Datum of 1988 (NAVD 88).

Horizontal coordinate information is referenced to the North American Datum of 1983 (NAD 83).

Geologic Framework and Hydrostratigraphy of the Edwards and Trinity Aquifers Within Northern Bexar and Comal Counties, Texas

By Allan K. Clark,[1] James A. Golab,[2] Robert R. Morris,[1] and Diana E. Pedraza[1]

Abstract

During 2020–22, the U.S. Geological Survey, in cooperation with the Edwards Aquifer Authority, revised a previous publication that described the geologic framework and hydrostratigraphy of the Edwards and Trinity aquifers within northern Bexar and Comal Counties, Texas. This report presents the refined maps and descriptions of geologic framework and hydrostratigraphy of the Edwards and Trinity aquifers within northern Bexar and Comal Counties that resulted from additional field data. Two informal geologic units and their corresponding informal hydrostratigraphic unit (HSU) names are introduced in this report; these informal units were identified during geologic mapping work done in counties adjoining the study area. Hydrostratigraphically, the rocks exposed in the study area represent a section of the upper confining unit to the Edwards aquifer, the Edwards aquifer, the upper zone of the Trinity aquifer, the middle zone of the Trinity aquifer, and the lower confining unit to the middle zone of the Trinity aquifer. The Washita, Eagle Ford, Austin, and Taylor Groups are generally considered to be the upper confining unit to the Edwards aquifer. The Edwards aquifer was subdivided into nine informally named HSUs (from top to bottom) as follows: I, II, III, IV, V, VI, VII, Seco Pass, and VIII. The upper zone of the Trinity aquifer was subdivided into five informal HSUs and two subunits (from top to bottom) as follows: cavernous, Camp Bullis, upper evaporite, fossiliferous (subunits: upper and lower), and lower evaporite. The middle zone of the Trinity aquifer was subdivided into nine named HSUs (from top to bottom) as follows: Bulverde, Little Blanco, Twin Sisters, Doeppenschmidt, Herff Falls (where present), Rust, Honey Creek, Hensell, and Cow Creek. The middle zone of the Trinity aquifer is underlain by the confining Hammett HSU. Groundwater recharge and flow paths in the study area are influenced not only by the hydrostratigraphic characteristics of the individual HSUs but also by faults and fractures.

Introduction

The Edwards and Trinity aquifers (fig. 1) are primary sources of water for agriculture, industry, and urban and rural communities in south-central Texas. Both the Edwards and Trinity are classified as major aquifers by the State of Texas (George and others, 2011). The population in northern Bexar and Comal Counties, Tex., is rapidly growing, thereby increasing demands on water resources (U.S. Census Bureau, 2022). To help water-resource managers, drinking-water suppliers, and policymakers effectively manage the water resources in the area, refined maps and descriptions of the geologic framework and hydrostratigraphic units (HSUs) of the aquifers in northern Bexar and Comal Counties are needed. For example, compared to the information available in previous reports, up-to-date detailed maps and descriptions of the hydrostratigraphic characteristics in northern Bexar and Comal Counties are needed by water-resource managers to identify areas in which urbanization of the recharge zone of the Edwards and Trinity aquifers might affect groundwater resources.

Groundwater flow and storage in the Edwards and Trinity aquifers are largely controlled by the geologic framework and hydrostratigraphy of the aquifers and by faulting and fractures (Kuniansky and Ardis, 2004); a refined characterization of these hydrogeologic features will be useful to water-resource managers who need to anticipate and mitigate issues related to changing land use and increasing groundwater demands. Hence, an initial characterization completed during 2014–16 (Clark and others, 2016b) was updated with additional field data during 2020–22 by the U.S. Geological Survey (USGS), in cooperation with the Edwards Aquifer Authority, to better document the geologic framework and hydrostratigraphy of the Edwards and Trinity aquifers within northern Bexar and Comal Counties.

Purpose and Scope

The purpose of this report is to present the geologic framework and hydrostratigraphy of the Edwards and Trinity aquifers within northern Bexar and Comal Counties, Tex. The

[1]U.S. Geological Survey.

[2]Texas Water Development Board.

report includes a detailed 1:24,000-scale hydrostratigraphic map, names, and descriptions of the geology and HSUs in the study area. The mapped HSUs (fig. 2) are intended to aid in identifying units that likely facilitate groundwater recharge or discharge or function as a confining layer. The scope of the report is focused on the geologic framework of the geologic units that contain the Edwards and Trinity aquifers and the hydrostratigraphy of the Edwards and Trinity aquifers within northern Bexar and Comal Counties. In addition, parts of the adjacent upper confining unit to the Edwards aquifer and lower confining unit to the middle zone of the Trinity aquifer are included.

Previous Studies and Background Information

Previous studies such as those by the USGS and the University of Texas, Bureau of Economic Geology, have mapped the geology, hydrostratigraphy, and structure in the study area at various scales. Examples of previous mapping include Barnes and others (1982), Collins (1991; 1992a, b, c; 1993a, b, c, d, e; 1994a, b, c, d; 1995a, b, c, d; 2000), Collins and others (1991), Raney and Collins (1991), Small and Hanson (1994), Stein and Ozuna (1995), and Clark and others (2009).

For this report, previously published hydrostratigraphic maps of the study area were updated by using onsite field mapping done with accurate, modern mapping tools such as highly accurate Global Positioning System (GPS) hand-held devices. The karstic geologic setting of northern Bexar and Comal Counties (U.S. Geological Survey, 2022a) underscores the need for updated hydrostratigraphic information. For example, the dissolution of the carbonate rocks composing the Edwards and Trinity aquifers (including those found in northern Bexar and Comal Counties) results in distinctive landforms rich in both springs and karst features (caves, sinkholes, and other visible areas of solutionally enlarged porosity). Porosity developed in carbonate rocks can have an appreciable effect on the hydrostratigraphic characteristics of the formations and can create focused points or areas of recharge and discharge (seeps and springs) (Hanson and Small, 1995). The same porosity that can focus recharge can also result in an aquifer that is highly susceptible to contamination because stormwater runoff is quickly transferred to the subsurface (Ryan and Meiman, 1996).

Description of Study Area

The study area covers approximately 866 square miles of northern Bexar County and Comal County, Tex. The upgradient part of the study area includes outcrops of the rocks that contain the Edwards and Trinity aquifers, and the downgradient part of the study area includes outcrops of the overlying confining units (Washita, Eagle Ford, Austin, and Taylor Groups) (fig. 1). The boundary of the study area coincides with the Comal County lines, except for the southern boundary. The southern boundary of the study area extends east and northeast from the western boundary of Bexar County to a few miles north of where Interstate 35 (I–35) crosses the northeastern boundary of the county. From there, the southern boundary of the study area arcs toward the northeast, a few miles northwest of and parallel to I–35 before it terminates at the Comal-Hays County line (fig. 1).

The rocks within the study area are sedimentary and range in age from Early to Late Cretaceous. Early Cretaceous rocks form the Trinity and Edwards Groups, and Late Cretaceous rocks form the Washita, Eagle Ford, Austin, and Taylor Groups (Barker and Ardis, 1996). The Miocene-age Balcones fault zone is the primary structural feature within the study area (fig. 1). The fault zone is an extensional system of faults that generally trends southwest to northeast in south-central Texas. The faults have normal throw, are en echelon, and are mostly downthrown to the southeast (Hill, 1900; Maclay and Small, 1986).

Methods of Investigation

The methods used in this study were similar to those used in Hanson and Small (1995), Stein and Ozuna (1995), Clark (2003, 2004), and Clark and others (2009, 2014, 2016a, b). Geologic data and previous reports were reviewed to assist in field mapping. During 2014–16, geologic and hydrostratigraphic mapping was performed in northern Bexar and Comal Counties on public and private lands. Field mapping techniques consistent with previous studies were used (Clark, 2003; Clark and Morris, 2015) and were aided by using GPS units and tablet-based digital maps and geologic mapping applications. Thicknesses of the mapped lithostratigraphic units and HSUs were derived from field observations. Thickness variations are from variations in local depositional and erosional conditions. Observations were recorded on site by using a tablet computer loaded with geospatially registered 7.5-minute USGS topographic maps. Locations of visible and interpreted contacts, faults and fractures, marker units, and other areas of interest were recorded by using the integrated third generation (3G) network assisted GPS receiver on the tablet computer. In areas without cellular service, positions were determined by using a handheld compass and triangulation techniques. Faults were identified in the field on the basis of observed and inferred stratigraphic offsets. Strike and dip of faults and fractures were also noted. Bedding attitudes of fractures and faults were obtained by using a hand-held compass or the tablet computer compass application. The data obtained by using the tablet-computer compass application were independently cross-verified daily with data obtained by using the hand-held compass. The field data were transferred by using ArcGIS ArcMap version 10.3.1 (Esri, 2016), quality checked by comparison with original draft maps, and then used to examine the geologic framework and develop the hydrostratigraphic map of the study area. The data that were

collected and compiled for this study, including the ArcGIS coverages derived from the data, are available in a companion data release (Pedraza and others, 2023).

Geologic names, HSU names, lithologic descriptions, and porosity type were based on information obtained from previous publications and field mapping associated with this study. The descriptions of the geologic framework and hydrostratigraphy in this report were adapted for the study area from Clark and others (2016a, b). Formal geologic names are consistent with those in the U.S. Geologic Names Lexicon (U.S. Geological Survey, 2022b). Informal geologic and HSU names are consistent with those used in previous publications (Rose, 1972; Maclay and Small, 1976; Clark and others, 2009, 2014, 2016a, b) (fig. 3). Two informal geologic units not identified in previous USGS reports were identified in this study, and their corresponding informal HSU names are introduced in this report: a geologic unit referred to as the burrowed member (Kkb) of the Kainer Formation of the Edwards Group (Seco Pass HSU) and a patch reef geologic unit (Kgrhf) of the lower member of the Glen Rose Limestone of the Trinity Group (Herff Falls HSU) (Rose, 1972; Perkins, 1974; Petta, 1977; Loucks and Kerans, 2003). These informal units were identified during geologic mapping work done in counties adjoining the study area. As greater thicknesses of the HSUs were observed in the new areas of study, it became evident that these units had been seen before, in the previously mapped areas, but their footprint was minimal in those areas and therefore not recognized.

It was recognized through the ongoing mapping in Bandera County, Tex., that a burrowed unit, first identified by Rose (1972), exists between the basal nodular and dolomitic members of the Kainer Formation of the Edwards Group. During mapping efforts to update previously mapped areas, it was recognized that the burrowed member exists in Bexar County but is thinner. Because the burrowed member can be mapped at the surface, the unit is now included as being present in Bexar County.

Although the presence of patch reefs in the lower member of the Glen Rose Limestone has been mentioned in geologic studies for decades (Perkins, 1974; Barnes and others, 1982), it was not until ongoing mapping in Bandera County and Kendall County, Tex., was completed that the full hydrostratigraphic importance of the patch reefs was recognized. A large portion of the patch reefs exists on private property, which rendered that portion inaccessible during previous mapping efforts. Recent mapping done for this report revealed that patch reefs are more abundant than previously thought, forming a continuous, albeit thin, depositional layer (band) that crosses several counties; the unit is traceable both in the surface and subsurface across Bandera, Kendall, Bexar, and Comal Counties.

Lithologic descriptions of carbonates were done according to the classification system of Dunham (1962). Descriptions of clastic rocks (sedimentary rocks composed of pieces of preexisting rocks) (Bates and Jackson, 1987) were done under the classification scale of Wentworth (1922).

HSUs were identified on the basis of variations in the amount and type of porosity visually evident in the outcrop. Porosity varies in each lithostratigraphic unit, depending on the original depositional environment, lithology, structural history, and diagenesis of the unit. Porosity type was described as either fabric selective or non-fabric selective based on the sedimentary carbonate classification system of Choquette and Pray (1970). Fabric-selective porosity is a result of original deposition or diagenetic changes in the sediments (Choquette and Pray, 1970). Non-fabric-selective porosity is a result of subsequent deformation or dissolution of the sediments (Choquette and Pray, 1970).

Sedimentological features, paleontology, and ichnofossils (tracks, trails, burrows, and other traces left by ancient life but not actual organism parts) (Hantzschel, 1962) were examined and described on site. Burrows formed by ancient marine animals represent a common ichnofossil observed in the study area during field mapping. Ichnofossils were described by using a combination of morphology, surface texture, and burrow-fill characteristics by following the techniques of Pemberton and Frey (1982). Ichnofabric indexes were recorded in the field and used to interpret the percentage of bioturbation as defined by Droser and Bottjer (1986). The term “bioturbation” originates from ichnology and refers to “churning and stirring of sediment by organisms” (Bates and Jackson, 1987, p. 71). The ichnofabric index is a semiqualitative field interpretation of the amount of bioturbation within strata (Golab and others, 2017). The ichnofabric index rates the amount of bioturbation on a scale from 1 to 6, where 1 represents a lack of any biological disturbance of the sediments that compose the formation and 6 represents sediments that were thoroughly homogenized because of biologic activity (Droser and Bottjer, 1986). The ichnofabric index was used in describing the measured geologic section at site 1 (figs. 1 and 4).

An outcrop of an intact geologic section (site 1) representing the middle zone of the Trinity aquifer was examined; in addition, a near-complete geologic core representing the middle zone of the Trinity aquifer and part of the upper zone of the Trinity aquifer (MW9–CC) obtained from Camp Stanley, San Antonio, Tex. (Blome and Clark, 2014), was also examined (fig. 1). The geologic section at site 1 was measured in the field by using a hand level and a Jacob’s staff. The near-complete core (MW9–CC) of the middle zone of the Trinity aquifer and the outcrop of the intact geologic section at site 1 were described lithologically, sedimentologically, paleontologically, and ichnologically (fig. 4).

Geologic Framework

In the study area, the Trinity Group (Imlay, 1940) rocks were deposited during the Early Cretaceous on a large, shallow marine carbonate platform (Comanche shelf, fig. 1) as clastic-carbonate “couplets” during three marine

transgressional events (Lozo and Stricklin, 1956; Stricklin and others, 1971) that caused the sea level to rise and shoreline to move inland. These three distinct "couplets" deposited sediments that formed (1) the Hosston and Sligo Formations (Imlay, 1940); (2) the Hammett Shale Member (Lozo and Stricklin, 1956) and the Cow Creek Limestone Member (Hill, 1901) of the Pearsall Formation (Imlay, 1940); and (3) the Hensell Sand Member (Hill, 1901) of the Pearsall Formation, as well as the lower and upper members of the Glen Rose Limestone (Hill, 1891).

The Early Cretaceous Edwards Group (Rose, 1972) rocks were deposited in an open marine to supratidal flats environment (Rose, 1972; Maclay and Small, 1986) during two marine transgressions. The rocks that compose the Edwards Group were deposited on the landward margin of the Comanche shelf, which was sheltered from storm waves and deep ocean currents by the Stuart City reef trend in the ancestral Gulf of Mexico (Clark and others, 2006) (fig. 1).

Following tectonic uplift, subaerial exposure, and erosion near the end of Early Cretaceous time, the area of present-day south-central Texas was again submerged during the Late Cretaceous by a marine transgression resulting in deposition of the Georgetown Formation of the Washita Group (Richardson, 1904). Much of the Georgetown Formation was subsequently removed during a marine regressive cycle (Curry, 1934). The Stuart City reef (fig. 1) was breached, resulting in deposition of the Del Rio Clay of the Washita Group (Rose, 1972). This transgressive episode continued through the deposition of the Buda Limestone of the Washita Group, Eagle Ford Group (Adkins, 1932), Austin Group (Murray, 1961), and Taylor Group (Hill, 1892) (fig. 3).

Trinity Group

The Trinity Group contains shale, mudstone to grainstone, boundstone, sandstone, and argillaceous limestone and is composed of the Hosston and Sligo Formations (neither of which is shown on fig. 3), the Pearsall Formation, and the Glen Rose Limestone (fig. 3). The basal Hosston and Sligo Formations of the Trinity Group were omitted from figure 3 because they are not present at land surface in the study area; these units will not be discussed further in this report.

Pearsall Formation

The Pearsall Formation of the Trinity Group consists of the Hammett Shale, Cow Creek Limestone, and Hensell Sand Members and typically ranged from 90 to 183 feet (ft) thick in the study area (fig. 3). Stratigraphically, the lowest mapped unit within the study area is the Hammett Shale Member of the Pearsall Formation. The Hammett Shale Member is approximately 50 ft thick (Clark and Morris, 2015). The lower 15 ft of the Hammett Shale Member contains siltstone and dolomite. The upper 35 ft is primarily claystone with siltstone lenses overlain by fossiliferous dolomitic limestone (Lozo and Stricklin, 1956; Wierman and others, 2010). The contact between the Hammett Shale Member and the overlying Cow Creek Limestone Member of the Pearsall Formation is conformable (Wierman and others, 2010).

The thickness of the Cow Creek Limestone Member of the Pearsall Formation ranges from 40 to 72 ft in the study area. Generally, the lower 14 ft of the Cow Creek Limestone Member is composed of dolomitic mudstone, wackestone, and packstone (coarsening upwards) with oysters throughout (Wierman and others, 2010). The upper part of the Cow Creek Limestone Member is brown to white, very fine-grained (approximately 0.0024–0.0049 inch [in.]) to fine-grained (approximately 0.0049–0.0098 in.) carbonate sand (grainstone) with localized crossbedding (Wierman and others, 2010).

The Hensell Sand Member of the Pearsall Formation ranges from 0 to 61 ft thick in the study area. The contact between the Cow Creek Limestone and Hensell Sand Members often contains a conglomerate or breccia of red sandstone. The Hensell Sand Member in Comal County grades southward from a claystone, siltstone, and terrigenous sand into a dolomitic limestone facies attributed to be the lower member of the Glen Rose Limestone. The Hensell Sand Member commonly contains oyster shells and quartz geodes. The contact between the Hensell Sand Member and the overlying Glen Rose Limestone is conformable (Sellards and others, 1932). In Hays County, Tex., just north of the current study area at The Narrows on the Blanco River (fig. 1), the Hensell Sand Member varies in thickness from 0 to 12 ft and was probably deposited as deltaic lobes (Clark and others, 2016a). East of The Narrows, the Hensell Sand Member is not present, and the Glen Rose Limestone overlies the Cow Creek Limestone directly. Field observations in the study area of the Hensell Sand Member noted that it often forms slopes and thick soils and supports lush grasses.

Glen Rose Limestone

The lower member of the Glen Rose Limestone of the Trinity Group commonly contains *Caprina* sp., Miliolida, *Orbitolina texana* (Roemer, 1852), *Toucasia* sp., *Trigonia* sp., *Turritella* sp., and various corals including *Astreopora*? *leightoni* (Wells, 1932) and *Orbicella whitneyi* (Wells, 1932). The lower member of the Glen Rose Limestone of the Trinity Group also contains trace fossil burrows, oysters, pectens, and shell fragments.

The lower part of the lower member of the Glen Rose Limestone contains 45–60 ft of resistive beds of wackestone to grainstone and boundstone (fig. 3) with burrows, *Caprina* sp., Miliolida, *Orbitolina texana* (Roemer, 1852), *Toucasia* sp., *Trigonia* sp., *Turritella* sp., pectens, and various corals and shell fragments. Above the 45–60 ft section of resistive beds of wackestone to grainstone and boundstone is approximately 40–70 ft of alternating beds of argillaceous wackestone to packstone, mudstone to grainstone, and miliolid grainstone (fig. 3). This 40–70 ft section is generally covered by soil

and vegetation where it outcrops (Clark and others, 2016a). Although the section is generally not visible in outcrops, ledges were identified that contained miliolid grainstone, grainstone, nodular bioturbated wackestone, and *Monopleura* sp. The 40–70 ft section also contains *Nerinea* sp., *Orbitolina texana* (Roemer, 1852), *Tylostoma* sp., and oysters, pectens, and pelecypods (Clark and others, 2016a).

Overlying the section of approximately 40–70 ft of alternating beds of argillaceous wackestone to packstone and mudstone to grainstone and of miliolid grainstone is a section approximately 40–80 ft thick that consists of relatively resistive mudstones to grainstone separated by argillaceous wackestone to packstone. The mudstone to grainstone beds in some locations interfinger laterally with boundstone (patch reefs) (Perkins, 1974; Loucks and Kerans, 2003). The patch reefs extend at least from the area near The Narrows in far western Hays County southwestward across southern Blanco and western Comal Counties to Camp Bullis in northern Bexar County and then west to the Pipe Creek area of Bandera County (Perkins, 1974; fig. 1). Fossil assemblages are similar to those in the underlying 40–70 ft section but also include *Requienia*, *Monopleura*, *Caprina*, and *Toucasia* spp.in the boundstone.

Above the 40–80 ft section is a 10–66 ft section of thick argillaceous wackestone, interspersed shale, thin shale beds, and occasional thin wackestone beds. This section commonly exhibits badlands-type weathering (intricately dissected topography with short steep slopes with narrow interfluves developed on surfaces with little or no vegetative cover) (Bates and Jackson, 1987) and often contains abundant *Orbitolina texana* (Roemer, 1852) with occasional gastropods and pelecypods. Some areas contain interfingering boundstone formed from rudist patch reefs and reefal talus that extends up from underlying sections (Perkins, 1974). The patch reefs are formed from *Requienia*, *Monopleura*, *Caprina*, and *Toucasia* spp.

Above the 10–66 ft section is a 30–40 ft section of resistive mudstones to wackestone with beds of argillaceous wackestone. Some areas contain interfingering boundstone formed from rudist patch reefs and reefal talus that extends up from underlying sections. The patch reefs (Perkins, 1974) are formed from *Requienia*, *Monopleura*, *Caprina*, and *Toucasia* spp. This section of the lower member of the Glen Rose Limestone often contains *Orbitolina texana* (Roemer, 1852), gastropods, pectens, and pelecypods (Clark and others, 2016a).

The uppermost section of the lower member of the Glen Rose Limestone is a 30–40 ft section of wackestone to grainstone, argillaceous wackestone, shales, and evaporites. This section contains occasional *Monopleura* sp. and *Toucasia* sp. (Clark and others, 2016a). The wackestone to grainstone grades upward into a bioturbated, nodular, fossiliferous wackestone named the "Salenia bed" by Whitney (1952). Common fossils in the Salenia bed are *Macraster* sp., *Nerinea* sp., *Orbitolina texana* (Roemer, 1852), *Porocystis globularis*, *Salenia texana*, gastropods, pectens, and pelecypods. The upper and lower members of the Glen Rose Limestone can be differentiated on the basis of a marker bed known as the *Corbula* marker bed. There are as many as three *Corbula* beds present at one location in the study area (sequentially stacked or separated by several feet), but only one *Corbula* bed (the lowermost one) is considered the marker bed. A detailed description of the *Corbula* beds found in the Glen Rose Limestone was provided in Clark and Morris (2015, p. 5):

> According to Lozo and Stricklin (1956) the *Corbula* bed is at the top of the lower member of the Glen Rose Limestone. This report considers the *Corbula* marker bed to be at the base of the upper member of the Glen Rose Limestone because three *Corbula* beds have been found in the study area. The marker bed is the lowest of three *Corbula* beds; the remaining two beds generally lay 2.5 and 5 ft above the marker *Corbula* bed. The stratotype location of the *Corbula* marker bed (Scott and others, 2007) is near the town of Blanco on the Blanco River * * * [fig. 1]. At the stratotype location sauropod tracks * * *, ripple marks and burrows can be found within the lower member of the Glen Rose Limestone [the sauropod tracks, ripple marks, and burrows were evident approximately 10 ft or less below the *Corbula* marker bed; Scott and others, 2007]. The *Corbula* marker bed, which is a grainstone, averages six inches thick and often contains ripple marks. The overlying *Corbula* beds are thin, often less than an inch thick, and usually contain more muds.

The upper member of the Glen Rose Limestone of the Trinity Group (fig. 3) thins towards northern Comal County because of variations in the depositional environment and erosion (Clark and others, 2016a). The upper member of the Glen Rose Limestone primarily consists of repeated coarsening upward sequences of argillaceous wackestone to grainstone (Clark and others, 2016a) and argillaceous limestone facies similar to the lower member of the Glen Rose Limestone but contains abundant evaporites and no rudist-dominated strata. Conditions during the deposition of the upper member of the Glen Rose Limestone never fully returned to the marine conditions of the lower member of the Glen Rose Limestone after the deposition of the *Corbula* bed (Fisher and Rodda, 1969) (fig. 3).

Immediately above the *Corbula* marker bed is a highly altered 8–10 ft thick section that originally contained evaporites that have been removed by dissolution; within this section are the previously mentioned overlying *Corbula* beds. This section contains crystalline limestone produced from alteration of the original rock matrix. The evaporite section also contains chalky mudstone, breccia, and boxwork voids where the evaporites have been dissolved. Where it outcrops, this section often has less woody vegetation (primarily *Juniperus ashei* [mountain cedar]) and thicker grasses such as *Muhlenbergia lindheimeri* (Lindheimer's muhly) (Hatch and others, 2016) compared to the vegetation growing over the outcrops of surrounding rocks (Clark and others, 2016a).

In the study area, a 120–150 ft thick section composed of alternating wackestone, packstone to miliolid grainstone, argillaceous limestone, and mudstone overlies the lower evaporite section. At the base of the 120–150 ft thick section is a thinly laminated silty mudstone with a "platy" appearance (Clark and others, 2009). *Hemiaster* sp., *Neithea* sp., *Orbitolina minuta* (Douglass, 1960), *Porocystis globularis*, *Protocardia texana*, *Tapes decepta*, and *Turritella* sp. are abundant. Near the top of this unit is a massive caprinid biostrome that, where present, is between 0 and 40 ft thick. The massive biostrome unit has been detected in the subsurface by using geophysical techniques at Camp Bullis in northern Bexar County (fig. 1) (Smith and others, 2005). In areas where the biostrome exists, the section containing the alternating wackestone, packstone to miliolid grainstone, argillaceous limestone, and mudstone is correspondingly thinner. The massive caprinid biostrome is primarily found in Bexar County and probably formed because of local variations in the depositional environment. In addition to the identified fossils, numerous unidentifiable gastropods are evident.

In the southern part of the study area, a second evaporite section is often present. The second evaporite section is not continuous over the entire study area but reaches a maximum thickness of 10 ft in the southern part of the study area. This upper evaporite section is formed from dissolved evaporites and consists of a highly altered crystalline limestone and chalky mudstone, often containing breccia and boxwork voids. The upper evaporite section thins northward and eastward across the study area and is absent in northern Comal County.

Overlying the second evaporite section is 120–150 ft of alternating beds of burrowed wackestone, with some packstone to miliolid grainstone, and argillaceous limestone. The argillaceous limestone is not well cemented and contains varying grain sizes.

The upper part of the upper member of the Glen Rose Limestone is 90–120 ft thick. This upper part contains evaporites, wackestone, packstone, miliolid grainstone, argillaceous limestone, and dolomitic limestone; it is also heavily bioturbated. Occasionally dinosaur tracks have been found near the contact of the Glen Rose Limestone and the overlying Kainer Formation of the Edwards Group (fig. 5).

Edwards Group

The Edwards Group (fig. 3), which overlies the Trinity Group (fig. 3), is composed of mudstone to grainstone, dolomitic mudstone, and chert. In the study area, the Edwards Group is composed of the Kainer and Person Formations (fig. 3). The Kainer Formation is subdivided into the following members (bottom to top): the basal nodular, burrowed, dolomitic, Kirschberg Evaporite, and grainstone (Rose, 1972; Maclay and Small, 1976). The Person Formation is subdivided into the following members (bottom to top): the regional dense, leached and collapsed (undivided), and cyclic and marine (undivided) (Maclay and Small, 1976). All members of the Kainer and Person Formations are informal except for the Kirschberg Evaporite (Rose, 1972; Maclay and Small, 1976; Small and Hanson, 1994; Stein and Ozuna, 1995).

Kainer Formation

The basal nodular member at the base of the Kainer Formation is typically 40–50 ft thick in the study area (fig. 3). The basal nodular member is a moderately hard, shaly, nodular, burrowed mudstone to miliolid grainstone and contains dolomite (Maclay and Small, 1976; Stein and Ozuna, 1995). According to Maclay and Small (1976, p. 25) "the basal nodular member also contains many stylolites, layers of wispy shales, and un-oxidized rock." The basal nodular member is a byproduct of bioturbation with subsequent compaction and can be identified in the field by gray mudstone containing "black rotund bodies (BRBs)—0.1 to 0.5 millimeter in diameter spherical, dark colored textural features of unknown origin" (Maclay and Small, 1986, p. 1). The basal nodular member also contains *Caprina* sp. (eastern part of the study area), *Ceratostreon texana* (formerly *Exogyra texana*, a type of saltwater oyster) (Stein and Ozuna, 1995; Clark, 2003; Scott and others, 2007), miliolids, and gastropods. The contact with the overlying burrowed member is conformable and gradational (Rose, 1972).

The burrowed member is 0–40 ft thick in the study area (fig. 3). The lower 20 ft of the burrowed member, where present, does not contain chert. According to Rose (1972, p. 32) the burrowed member is composed of "* * * massive, resistant layers of porous, burrowed limestone. The beds consist of mudstone and wackestones."

The dolomitic member is typically 50–120 ft thick in the study area (fig. 3). The lower 20 ft of the dolomitic member, where the burrowed member is absent, does not contain chert. Chert is found as beds and as nodules throughout the Edwards Group above this lower 20 ft of the dolomitic member. According to Maclay and Small (1976, p. 24), the dolomitic member is "* * * a hard, dense to granular, dolomitic limestone that contains scattered cavernous layers." They further differentiate the dolomitic member, stating that the lower three-fourths of the dolomitic member is composed of sucrosic dolomites and grainstones, with hard, dense limestones interspersed, and that the upper one-fourth of the dolomitic member is composed mostly of hard, dense mudstone, wackestone, packstone, grainstone, and recrystallized dolomites (Maclay and Small, 1976) with bioturbated beds. The contact between the dolomitic member and the overlying Kirschberg Evaporite Member is conformable.

The Kirschberg Evaporite Member is typically 40–50 ft thick in the study area and is a highly altered crystalline limestone and chalky mudstone with occasional grainstone associated with tidal channels, all of which contain chert (Maclay and Small, 1976) both as beds and as nodules (fig. 3). Boxwork molds, which are associated with the removal of evaporites, are common, and "the matrix of the boxwork has

recrystallized to a coarse grain[ed] spar" (Maclay and Small, 1976, p. 24). The Kirschberg Evaporite Member also contains intervals of collapse breccia and travertine deposits (Maclay and Small, 1976). The contact with the overlying grainstone member is unconformable.

The grainstone member is typically 40–50 ft thick in the study area and is a hard, dense limestone that consists mostly of a tightly cemented miliolid or skeletal fragmented grainstone (Maclay and Small, 1976) (fig. 3). The member also contains interspersed chalky mudstone and wackestone (Maclay and Small, 1976) and chert, both as beds and as nodules. Crossbedding and ripple marks are common primarily at the contact with the overlying regional dense member. The contact between the grainstone and regional dense members is conformable.

Person Formation

The regional dense member of the Person Formation is a dense, shaly limestone that is typically 20–24 ft thick in the study area (fig. 3). Maclay and Small (1976) described the regional dense member of the Person Formation as an oyster-shell mudstone and iron wackestone containing wispy shale partings. It also contains wispy iron-oxide stains with chert nodules being rarer than in the rest of the chert-bearing Edwards Group.

The leached and collapsed members (undivided) are typically 70–90 ft thick in the study area and consist of a hard, dense, recrystallized limestone composed of mudstone, wackestone, packstone, and grainstone; chert is present throughout (Maclay and Small, 1976; Stein and Ozuna, 1995) (fig. 3). The leached and collapsed members are heavily bioturbated with iron-stained beds (Stein and Ozuna, 1995) separated by more massive limestone beds. The leached and collapsed members are often stromatolitic and contain chert both as beds and as large nodules. *Toucasia* sp. and fragments are often found just above the contact with the underlying regional dense member. Although rare, the coral *Montastrea roemeriana* and oysters can be found (Finsley, 1989).

The cyclic and marine members (undivided) are typically 80–90 ft thick in the study area (fig. 3). The undivided cyclic and marine members were mapped and considered as one unit. Maclay and Small (1976) stated that the cyclic and marine members are locally bioturbated and are mostly composed of pelletal limestone that ranges from chalk to mudstone, as well as of miliolid grainstone. A packstone containing large caprinids also is present near the contact with the overlying Georgetown Formation. Chert is common both as beds and as large nodules. Some of the caprinids identified in the field were several feet long and as much as 5 in. in diameter. The cyclic and marine members are composed of thin to massive beds; some crossbedding is evident. According to Maclay and Small (1976), the Georgetown Formation overlies the Person Formation of the Edwards Group unconformably.

Washita Group

The Georgetown Formation of the Washita Group is typically 20–30 ft thick in the study area and is a reddish-brown, gray to light tan, shaly mudstone and wackestone (fig. 3). It commonly contains black dendrites, iron nodules, and iron staining and often resembles the Buda Limestone. The Georgetown Formation is often fossiliferous with *Plesioturrilites brazoensis* and *Waconella wacoensis* common. *Waconella wacoensis* is the index fossil for the Georgetown Formation. The Del Rio Clay overlies the Georgetown Formation unconformably.

The Del Rio Clay of the Washita Group is typically 40–50 ft thick in the study area. It is a fossiliferous blue-green to yellow-brown clay with thin beds of packstone (fig. 3). The Del Rio Clay of the Washita Group contains iron nodules and the index fossil *Ilymatogyra arietina*. The contact between the Del Rio Clay and the overlying Buda Limestone is unconformable (Martin, 1967) and easily recognized, with the Buda Limestone blocks often slumping down hillsides over the Del Rio Clay outcrops (Clark and others, 2013).

The Buda Limestone of the Washita Group is approximately 40–50 ft thick in the study area and is buff to light-gray, dense nodular mudstone and wackestone containing calcite-filled veins and bluish dendrites (fig. 3). It is a porcelaneous limestone that weathers from a smooth gray to a grayish white; its nodular surface has conchoidal fractures (Adkins, 1932). The Buda Limestone commonly contains iron nodules, iron staining, and shell fragments. The contact with the overlying Eagle Ford Group is unconformable (Martin, 1967).

Eagle Ford Group

The Eagle Ford Group (undivided) is approximately 20–40 ft thick in the study area and consists of brown, flaggy, sandy shale and argillaceous limestone (Trevino, 1988) (fig. 3). In the study area, this group contains iron nodules, the fossil *Inoceramus* sp., shark teeth, and fossil fragments. Some of the freshly fractured flagstones emit a petroliferous odor. The upper contact with the overlying Austin Group is unconformable (Denne and others, 2016).

Austin Group

The Austin Group (undivided) is 130–160 ft thick in the study area and consists of massive, chalky, locally marly mudstone (Small, 1986; Hanson and Small, 1995; Maclay, 1995) containing intervals of nodular (bioturbated) wackestone. The Austin Group commonly contains iron nodules. The fossils *Gryphaea aucella* and *Inoceramus* sp. (Banta and Clark, 2012) are common. The Austin Group also contains varying amounts of volcaniclastics and terrigenous clastics (Martinez, 1982). The fractures often contain void-filling calcite, sometimes in the form of dogtooth spar. The contact with the overlying Taylor Group is unconformable (Martinez, 1982).

Taylor Group

In the study area the Taylor Group (undivided) is composed of the Pecan Gap Chalk. According to Arnow (1963), the Taylor Group is approximately 230–540 ft thick in Bexar County, thickening southward. The formation is mostly marl and calcareous clay and is blue in the subsurface but weathers to a greenish yellow where it is exposed at land surface. Fossils are common, the most notable being the large *Exogyra ponderosa* (Arnow, 1963).

Structural Features

The principal structural feature in northern Bexar and Comal Counties is the Balcones fault zone (fig. 1), which is the result of Miocene-age faulting (Weeks, 1945**)** and fracturing. As is typical elsewhere in the Balcones fault zone, most of the faults in the study area are high-angle to nearly vertical, en echelon, normal faults that are downthrown to the southeast (fig. 6) (George, 1952). As with any normal fault extensional system, the geologic structure in this area also includes horst and graben structures (Pantea and others, 2014).

The structurally complex Balcones fault zone contains relay ramps (Hovorka and others, 1996), which are a common feature formed during the growth of normal and extensional fault systems (Hus and others, 2005). Several reports provide detailed descriptions of relay ramps and relay ramp development in the Balcones fault zone; these include but are not limited to Hovorka and others (1996), Collins and Hovorka (1997), Ferrill and others (2003), Faith (2004), and Clark and Journey (2006). Relay ramps form in extensional fault systems to allow for deformation changes along the fault block (Clark and Journey, 2006). Ramp structures connect the footwall of a fault segment to the stratigraphically higher segment (hanging wall) of the overlapping fault. As stress (extension) occurs and strain along the ramp increases, rotation and internal fracturing occur along the relay ramp (Trudgill, 2002). Subsequently, continuing extension produces cross faults within the relay ramp structure.

The primary orientation of mapped fractures and faults in the study area is southwest to northeast between 45 and 50 degrees. The conjugant fractures trend perpendicular to the Balcones fault zone at approximately 145–150 degrees. Variation in strikes and dips of the faults in the outcrop is a result of stress-strain relations of the different lithologies of the rocks (Trudgill, 2002; Ferrill and others, 2003; Clark and others, 2014).

Hydrostratigraphy

Hydrostratigraphically the rocks exposed in the study area represent a section of the upper confining unit to the Edwards aquifer, the Edwards aquifer, the upper zone of the Trinity aquifer, the middle zone of the Trinity aquifer, and the Hammett Shale (fig. 3). In the study area the Edwards aquifer is contained in the Georgetown Formation and in the rocks forming the Edwards Group. The Trinity aquifer is contained in the rocks forming the Trinity Group. The Edwards and Trinity aquifers are karstic with secondary permeability and porosity associated with bedding planes, fractures, and caves (Maclay and Small, 1983; Johnson and others, 2002; Ferrill and others, 2003; Gary and others, 2011). The following descriptions of the hydrostratigraphy and porosity of individual HSUs are modified and expanded from Choquette and Pray (1970), Maclay and Small (1976), Stein and Ozuna (1995), Clark and others (2009), Blome and Clark (2014), and Clark and Morris (2015).

Upper Confining Unit to the Edwards Aquifer

The Pecan Gap Chalk (Kpg), Austin Group (Ka), Eagle Ford Group (Kef), Buda Limestone (Kb), and Del Rio Clay (Kdr) collectively are generally considered to be the upper confining unit to the Edwards aquifer (Maclay and Small, 1976; Hanson and Small, 1995) (fig. 3). Because the formations and groups are generally categorized as a confining unit to the Edwards aquifer and not as separate water-bearing aquifers, the lithologic terms (group, formation, limestone, and clay) will hereinafter be used to describe both the geologic framework and hydrologic characteristics of the HSU being described. The upper confining unit to the Edwards aquifer does not supply appreciable amounts of water to wells in the study area except for the Austin Group (Petitt and George, 1956); for this reason, of the units that compose the upper confining unit to the Edwards aquifer, only the Austin Group will be described.

The Austin Group supplies water to several springs in the study area, as well as some domestic and irrigation wells (Garza, 1962; Arnow, 1963; Banta and Clark, 2012). The most prolific wells and springs within the Austin Group likely tap water that moves up faults and fractures under artesian conditions from the underlying Edwards aquifer (Veni, 1988; Banta and Clark, 2012).

Edwards Aquifer

The Edwards aquifer was subdivided into HSUs I to VIII by Maclay and Small (1976) (fig. 3). A ninth informal HSU (Seco Pass HSU) was added on the basis of additional field observations made by the authors in counties adjoining the study area. The Georgetown Formation of the Washita Group contains HSU I (Kg). The Person Formation of the Edwards Group contains HSUs II (cyclic and marine members, undivided [Kpcm]), III (leached and collapsed members, undivided [Kplc]), and IV (regional dense member [Kprd]), and the Kainer Formation of the Edwards Group contains HSUs V (grainstone member [Kkg]), VI (Kirschberg Evaporite

Member [Kkke]), VII (dolomitic member [Kkd]), Seco Pass (burrowed member [Kkb], where present), and VIII (basal nodular member [Kkbn]).

Barker and Ardis (1996, p. B42) wrote, "the Edwards aquifer primarily is recharged by (1) seepage from streams draining the Hill Country, where the streams flow onto permeable outcrop areas of the Edwards Group and Devils River Formation (Puente, 1978); (2) infiltration of precipitation on the outcrop areas; (3) subsurface inflow across the up-dip margin of the Balcones fault zone where the Trinity aquifer is laterally adjacent to down-faulted Edwards strata (Veni, 1994); and (4) diffuse upward leakage from the underlying Trinity aquifer."

Hydrostratigraphic Unit I (Kg)

HSU I is considered part of the Edwards aquifer (fig. 3), but hydrologically it functions as a confining unit (George, 1952; Maclay and Small, 1976; Hanson and Small, 1995). Porosity is generally fabric selective formed by isolated molds surrounded by a rock matrix. According to Maclay and Small (1976), HSU I contains porosity of less than 5 percent. Maclay and Small (1976) further stated that the capillary forces of the small voids do not allow the rocks to drain by gravity. Arnow (1959) considered HSU I to be part of the Edwards aquifer because this unit is the primary target used by water-well drillers when setting well casings. George (1952), Land and Dorsey (1988), Blome and others (2005), and Clark and others (2006) have considered this unit as part of the upper confining unit to the Edwards aquifer. Stein and Ozuna (1995) stated that the Georgetown Formation is not known to produce water.

Hydrostratigraphic Unit II (Kpcm)

HSU II (fig. 3) contains less than 15 percent porosity in the form of fabric-selective molds and burrows and non-fabric-selective fractures (Maclay and Small, 1976). Hanson and Small (1995) observed that HSU II also contains non-fabric-selective vug porosity. Field observations show burrow porosity associated with bioturbation in the form of a cylindrical, T-branched boxwork network of interconnected burrows (*Thalassinoides*) made by a genus known only by the trace fossils they left behind (Ehrenberg, 1944; Seilacher, 2007). In addition, the unit has non-fabric-selective porosity associated with bedding planes and caves. Hanson and Small (1995) also noted that the unit is water bearing, although field observations during the study documented in this report indicate that HSU II has only slightly less porosity than HSU III.

Hydrostratigraphic Unit III (Kplc)

HSU III (fig. 3) has a reported porosity of 20 percent, which makes it the most porous and permeable part of the upper part of the Edwards aquifer (Person Formation) (Maclay and Small, 1976). HSU III contains fabric-selective burrow and bedding plane porosity. It also contains non-fabric-selective vug, breccia, fracture, and cave porosity. The fabric-selective burrow porosity is associated with bioturbated zones (characterized by *Thalassinoides*). Maclay and Small (1976) associated the breccia and cave porosity with the collapsed zones resulting from dissolution of evaporites. In addition, Hanson and Small (1995) stated that many of the springs in south-central Texas, such as Comal Springs (fig. 1), issue from faults that are believed to be near the base of the HSU III. The unit is water bearing and has the highest reported porosity in the upper part of the Edwards aquifer.

Hydrostratigraphic Unit IV (Kprd)

HSU IV (fig. 3) has less than 5 percent porosity and yields no water (Maclay and Small, 1976). This HSU is likely the least porous or permeable unit of the Edwards aquifer and locally might be a confining unit (Hanson and Small, 1995). According to Stein and Ozuna (1995), it probably is an effective vertical confining unit between HSU III and HSU V (fig. 3); however, non-fabric-selective fracture and cave porosity are present in the unit, which might greatly reduce the confining effects of this HSU in some areas. All caves known in this HSU are vertical shafts, often with major horizontal cavern development either above or below the unit (Veni, 2005).

Hydrostratigraphic Unit V (Kkg)

HSU V (fig. 3) has a reported porosity of less than 10 percent (Maclay and Small, 1976) with minor fabric-selective interparticle, intergranular, and bedding plane porosity (Hanson and Small, 1995). The unit also contains non-fabric-selective fracture and cave porosity (Maclay and Small, 1976). Maclay and Small (1976) reported that the middle of the unit contains a fabric-selective burrow porosity that has resulted in the development of non-fabric-selective cave porosity.

Hydrostratigraphic Unit VI (Kkke)

HSU VI (fig. 3) is the most porous and permeable unit in the lower part of the Edwards aquifer (Kainer Formation) with porosity of more than 20 percent that occurs in several forms (Maclay and Small, 1976; Barker and others, 1994). The unit has abundant fabric-selective intergranular and moldic porosity and non-fabric-selective vug, fracture, breccia, and cave porosity. The moldic porosity is often in the form of "boxwork" voids caused by the dissolution of evaporites and the deposition of secondary neospar and travertine (Hanson and Small, 1995). Fracture porosity is associated with faulting, and breccia porosity is associated with the removal of evaporites (Maclay and Small, 1976).

Hydrostratigraphic Unit VII (Kkd)

The porosity of HSU VII (fig. 3) ranges from 5 to 20 percent; fabric-selective and non-fabric-selective porosity are present (Maclay and Small, 1976). The fabric-selective porosity consists of interparticle, intergranular, intercrystalline, moldic, burrow, and bedding plane porosity. The non-fabric-selective porosity consists of vug, fracture, and cave porosity (Maclay and Small, 1976). Moldic and burrow porosity are common within the bioturbated beds riddled by interconnected *Thalassinoides* (Ehrenberg, 1944; Seilacher, 2007). In one location, *Skolithos* burrows (fig. 7) can be seen in the outcrop; the *Skolithos* burrows are not interconnected to other burrows (Seilacher, 2007). HSU VII is water bearing and according to Veni (2005) forms some of the deepest vertical pits in Texas.

Hydrostratigraphic Unit Seco Pass (Kkb)

The porosity of the Seco Pass HSU (fig. 3), where present, consists of both fabric-selective and non-fabric-selective porosity and reportedly ranges from 5 to 20 percent (Rose, 1972; Maclay and Small, 1976). On the basis of field observations made by the authors, the porosity in this HSU might be appreciably higher than the reported maximum of 20 percent because of the extensive amount of interconnected burrows. The fabric-selective porosity consists of interparticle, intergranular, intercrystalline, moldic, and interconnected burrow porosity. The non-fabric-selective porosity consists of fracture, bedding plane, channel, and cave porosity. Interconnected *Thalassinoides* burrow porosity was observed within the bioturbated beds by the authors of this report. HSU Seco Pass is water bearing; according to Rose (1972, p. 34), "The burrowed member [Seco Pass HSU] is the chief water-bearing zone of the Edwards (in the subsurface). The porosity is the result in part of preferential leaching and removal of burrow-fillings, producing superb honeycomb porosity * * *." Barker and others (1994, p. 38) further stated that the burrowed member "* * * near the base of the formation, may be the most permeable part of the Edwards Group * * *."

Hydrostratigraphic Unit VIII (Kkbn)

HSU VIII (fig. 3) has a porosity of less than 10 percent (Maclay and Small, 1976); it contains fabric-selective interparticle, moldic, burrow, and bedding plane porosity and non-fabric-selective fracture and cave porosity. The unit is probably best described as a semiconfining unit; the degree to which it functions as a confining unit likely depends on the amount of interconnected burrow porosity and cave porosity (Clark and others, 2016a). According to Veni (2005), HSU VIII contains some of the largest cave chambers and passages in the study area. These cave features were probably formed by dissolution processes as groundwater reacted with highly bioturbated beds within the unit or in the underlying cavernous unit (Veni, 2005).

Trinity Aquifer

Ashworth (1983) subdivided the Trinity aquifer into upper, middle, and lower aquifer units (hereinafter referred to as "zones"). The upper zone of the Trinity aquifer is contained in the upper member of the Glen Rose Limestone (fig. 3). The upper zone of the Trinity aquifer is subdivided into the cavernous (Kgrc), Camp Bullis (Kgrcb), upper evaporite (Kgrue), fossiliferous (Kgrf; upper [Kgruf] and lower [Kgrlf] subunits), and lower evaporite (Kgrle) HSUs (fig. 3). The middle zone of the Trinity aquifer is contained in the lower member of the Glen Rose Limestone, Hensell Sand, and Cow Creek Limestone (fig. 3).

The HSUs that contain the middle zone of the Trinity aquifer consist of (top to bottom) the Bulverde (Kgrb), Little Blanco (Kgrlb), Twin Sisters (Kgrts), Doeppenschmidt (Kgrd), Herff Falls (Kgrhf, where present), Rust (Kgrr), Honey Creek (Kgrhc), Hensell (Kheh), and Cow Creek (Kcccc) HSUs (fig. 3). Because the Herff Falls HSU is formed within a series of patch reefs that trend in a specific zone through the study area, it is not present in all locations and is equivalent in age to the Little Blanco, Twin Sisters, and Doeppenschmidt HSUs (fig. 3). The underlying Hammett (Khah) HSU is a regional confining unit between the middle and lower zones of the Trinity aquifer. The lower zone of the Trinity aquifer is not exposed in the study area.

According to Barker and Ardis (1996), the Trinity aquifer is recharged, in order of importance (most to least), by lateral subsurface inflow of groundwater from the Edwards Plateau, infiltration of precipitation on the outcrop, and seepage of surface water from shallow, tributary streams. Ashworth (1983) stated that sinkholes in streambeds in the Glen Rose Limestone frequently intercept surface water to provide substantial amounts of recharge to the Trinity aquifer. Fractures and faults, as well as various other types of porosity, link the upper, middle, and lower zones of the Trinity aquifer and result in a "leaky-aquifer system" (Ashworth and others, 2001, p. 8).

Upper Zone of the Trinity Aquifer

The upper zone of the Trinity aquifer was informally subdivided into five HSUs by Clark (2003) that were subsequently informally renamed by Clark and others (2009). These five HSUs are (top to bottom) the cavernous (Kgrc), Camp Bullis (Kgrcb), upper evaporite (Kgrue), fossiliferous (Kgrf; upper [Kgruf] and lower [Kgrlf] subunits), and lower evaporite (Kgrle) (fig. 3).

Cavernous Hydrostratigraphic Unit (Kgrc)

The cavernous HSU (fig. 3) is a water-bearing unit approximately 90–120 ft thick with fabric-selective porosity associated with molds, burrows, and bedding planes. Non-fabric-selective porosity within the cavernous HSU is in the form of fractures and caves. The cavernous HSU contains

beds that were once evaporites; these beds have moldic (boxwork) and breccia porosity. The cavernous HSU contains evaporite beds along with large amounts of bioturbation that includes beds of *Thalassinoides* (Clark and others, 2016a; Golab and others, 2017) and rhizocretions (fig. 8), which are "pedodiagenetic mineral accumulations around plant roots" (Klappa, 1980, p. 615). The bioturbated beds have resulted in interconnected lateral flow linking bedding planes, fractures, and caves. Field observations indicate that cavernous HSU is more porous than the underlying Camp Bullis HSU. The cavernous HSU, however, has a small lateral extent and is not present at the surface through most of the study area (Clark and Morris, 2015). The high permeability of the overlying Edwards aquifer has introduced meteoric water into faults and fractures, thereby creating karstic groundwater flow paths that continue into the Trinity aquifer from the Edwards aquifer (Clark, 2004; Smith and others, 2005). Johnson and others (2010) have shown through dye tracing that the cavernous HSU of the upper zone of the Trinity aquifer is hydrologically indistinguishable from the Edwards aquifer. The cavernous HSU functions as part of the Edwards aquifer because of the lack of intervening confining beds. This hydrologic connection has further been enhanced by faulting of the cavernous HSU against parts of the Edwards aquifer.

Camp Bullis Hydrostratigraphic Unit (Kgrcb)

The Camp Bullis HSU (fig. 3) is approximately 120–150 ft thick in the study area. Fabric-selective burrow and bedding plane porosities and non-fabric-selective fracture porosity are the primary porosity types identified in the field. Some cave development, which was likely caused by the intersection of fractures with bedding planes, has been observed. Most of the observed Camp Bullis HSU has little solution enlargement of fractures and is considered a confining unit (Clark, 2004; Clark and Morris, 2015). Field observations indicate that beds in the Camp Bullis HSU likely prevent appreciable vertical fluid flow but instead perch groundwater on less soluble beds. This perched groundwater is likely transmitted laterally through bioturbated beds consisting of *Thalassinoides* and *Ophiomorpha* (Clark and others, 2016a), therefore resulting in conduits and caves that yield water to seeps and springs.

Upper Evaporite Hydrostratigraphic Unit (Kgrue)

The upper evaporite HSU (fig. 3) is not continuous throughout the study area; however, where present it can be as much as 10 ft thick. The upper evaporite HSU contains fabric-selective interparticle, moldic (boxwork), and burrow porosity and non-fabric-selective collapsed breccia porosity. The extensive bioturbation of this unit aided in the development of the fabric-selective porosity (Fisher and Rodda, 1969). This HSU is considered water bearing and diverts groundwater laterally to discharge at springs and seeps (Clark, 2004; Clark and others, 2009).

Fossiliferous Hydrostratigraphic Unit (Kgrf Upper [Kgruf] and Lower [Kgrlf] Subunits)

The fossiliferous HSU (fig. 3) can be subdivided in some locations into upper and lower subunits. The fossiliferous HSU (undivided) has a total thickness of 120–150 ft in the study area. In areas where the fossiliferous HSU could not be divided, it is identified as Kgrf on figures 2 and 3. Where present, the upper subunit can be as much as 40 ft thick. The upper subunit of the fossiliferous HSU is found only in the southern and western parts of the study area. The upper fossiliferous subunit contains extensive non-fabric-selective fracture and cave porosity and fabric-selective moldic and burrow porosity (Clark, 2003). This subunit contains numerous caves that readily transport water long distances, some of which discharges at springs (Clark, 2003).

In areas where the upper fossiliferous subunit is present, the lower fossiliferous subunit has a thickness of 80–110 ft. The lower subunit of the fossiliferous HSU contains fabric-selective moldic and burrow porosity and non-fabric-selective fracture porosity (Clark, 2003). The lower subunit of the fossiliferous HSU is generally considered a confining unit (Clark, 2003; Clark and others, 2009).

Lower Evaporite Hydrostratigraphic Unit (Kgrle)

The lower evaporite HSU (fig. 3) is approximately 8–10 ft thick in the study area and contains fabric-selective interparticle, moldic (boxwork), and burrow porosity. It also contains non-fabric-selective breccia porosity. According to Fisher and Rodda (1969), the extensive bioturbation of the lower evaporite HSU aided in the development of the fabric-selective porosity. The lower evaporite HSU is water bearing and discharges laterally along its contact with the underlying Bulverde HSU at springs and seeps (Clark, 2003; Clark and others, 2009).

Middle Zone of the Trinity Aquifer

The middle zone of the Trinity aquifer is contained in the Bulverde, Little Blanco, Twin Sisters, Doeppenschmidt, Herff Falls (where present; figs. 3, 9, and 10), Rust, Honey Creek, Hensell, and Cow Creek HSUs (Clark and Morris, 2015). Because the Herff Falls HSU is formed within a series of patch reefs that trend along a specific zone through the study area, it is not present in all locations and is equivalent in age to the Little Blanco, Twin Sisters, and Doeppenschmidt HSUs. Underlying the Cow Creek HSU is the regional confining unit, the Hammett HSU, separating the middle and lower zones of the Trinity aquifer. Within the Trinity aquifer, the middle zone is the primary source of water production for both public and domestic wells.

Bulverde Hydrostratigraphic Unit (Kgrb)

The Bulverde HSU (fig. 3) is the uppermost unit of the middle zone of the Trinity aquifer. The Bulverde HSU is typically 30 ft thick in the study area, but its thickness can range from 30 to 40 ft. It contains fabric-selective moldic porosity associated with bioturbation and bedding plane porosity. The Bulverde HSU also contains non-fabric-selective breccia porosity formed from the dissolution of evaporites (Clark and others, 2016a) and fracture porosity. The shale bed (which is several feet thick) at the top of the unit is a confining unit and restricts the downward migration of water, which results in water moving laterally to discharge as seeps and springs. Field observations indicate that this unit is a confining unit and is often used for constructing stock ponds.

Herff Falls Hydrostratigraphic Unit (Kgrhf)

The Herff Falls HSU (fig. 3) is estimated to be 0–90 ft thick in the study area and is formed within patch reefs and reefal talus. It contains both fabric-selective moldic and burrow porosity and non-fabric-selective bedding plane, fracture, channel, and cave porosity. On the basis of evidence from field observations and previous studies (Williams and others, 1952; Puente, 1978; Veni, 2021), the Herff Falls HSU is likely a primary water-bearing unit of the middle Trinity aquifer. The Herff Falls HSU contains extensive porosity, which is enhanced by the presence of interconnected sinkholes and caves. Puente (1978) demonstrated that the Cibolo Creek watershed contributes substantial recharge to the groundwater system. The substantial amount of recharge can be seen in field observations of sinkhole formations within the Cibolo Creek streambed at Herff Falls (Veni, 2021) (fig. 1), is described in previous studies (Williams and others, 1952, p. 58–59; Puente, 1978; Ockerman, 2007), and is supported by anecdotal accounts such as the observations of whirlpools near Herff Falls. Whirlpools mark locations of rapid recharge and have been observed by the authors and other researchers while they were doing field work along Cibolo Creek near Herff Falls after large storm events. From hydrogeologic evidence in previous publications (Williams and others, 1952; Puente, 1978; Veni, 2021) and field observations made during this study, the authors of this report suspect that most of the surface-water losses along Cibolo Creek are likely to occur within the Herff Falls HSU because of its extensive porosity and the presence of interconnected sinkholes and caves.

Little Blanco Hydrostratigraphic Unit (Kgrlb)

The Little Blanco HSU (fig. 3) is typically 30 ft thick in the study area but can range in thickness from 30 to 40 ft. It contains both fabric-selective moldic, burrow, and bedding plane porosity and non-fabric-selective fracture porosity. According to Golab and others (2017), fabric-selective *Thalassinoides* and other biogenic porosity have likely created a network of interconnected porosity resulting in increased permeability that is a major component of this unit's ability to transmit water. Several caves and underground streams were identified in this HSU by the authors of this report during their field work, consistent with observations made earlier by another researcher that worked in the same area (George Veni, National Cave and Karst Research Institute, written commun., 2016). The Little Blanco HSU is considered water bearing in the study area.

Twin Sisters Hydrostratigraphic Unit (Kgrts)

The Twin Sisters HSU (fig. 3) is typically 30 ft thick in the study area but can range in thickness from 10 to 66 ft. It contains fabric-selective interparticle porosity. In the study area, the shale beds within the Twin Sisters HSU function as a semiconfining unit (Clark and others, 2016a). Water in the unit moves laterally, resulting in discharge from seeps and springs along hillsides providing water to numerous stock ponds (Clark and Morris, 2015).

Doeppenschmidt Hydrostratigraphic Unit (Kgrd)

The Doeppenschmidt HSU (fig. 3) can range from approximately 40 to 80 ft thick in the study area but typically is about 40 ft thick. It contains fabric-selective interparticle, moldic, burrow, and bedding plane porosity and may contain non-fabric-selective fracture and cave porosity. There are seeps and springs near the basal contact with the underlying Rust HSU. The Doeppenschmidt HSU grades laterally into patch reefs that contain appreciable interconnected moldic porosity formed by *Caprina* sp. In addition, it contains some bioturbated beds that may link fabric-selective and non-fabric-selective porosity, which could result in increased permeability and enhance its ability to transmit water rapidly (Clark and others, 2016a; Golab and others, 2017). The Doeppenschmidt HSU is water bearing in the study area.

Rust Hydrostratigraphic Unit (Kgrr)

The Rust HSU (fig. 3) is approximately 40–70 ft thick in the study area but typically it is 40 ft thick. It contains fabric-selective interparticle porosity and non-fabric-selective fracture, channel, and cave porosity. Fracture porosity is not well developed, but several of the thicker limestone beds have fractures with solution enlargement. The unit contains cave and channel porosity primarily near faults; most caves probably formed because of roof collapse of caves in the underlying Honey Creek HSU. The Rust HSU appears to function as a semiconfining unit in nonfaulted areas (Clark and others, 2016a) because springs and seeps occur near the upper contact with the overlying Doeppenschmidt HSU, which would necessitate restricted vertical flow through the unit. The unit contains bioturbated beds of *Paleophycus* and *Planolites*, but the bioturbated beds do not increase fabric-selective biogenic porosity to the same degree as in other, more transmissive HSUs (Clark and others, 2016a; Golab and others, 2017).

Honey Creek Hydrostratigraphic Unit (Kgrhc)

The Honey Creek HSU (fig. 3) is approximately 45–60 ft thick but is typically 55 ft thick; it is the basal unit of the lower member of the Glen Rose Limestone. The Honey Creek HSU contains fabric-selective interparticle, moldic, burrow, and bedding plane porosity. Fabric-selective burrow porosity is primarily from *Paleophycus* with some *Thalassinoides* networks (Clark and others, 2016a; Golab and others, 2017). While defined as an aquifer unit, most of the biogenic porosity of the Honey Creek HSU appears to be restricted to the lower half of the unit. It also contains non-fabric-selective fracture, channel, and cave porosity. Most fracture and karstic development occurs in the lower parts of the Honey Creek HSU (Clark and Morris, 2015), which probably reflects the importance of the biogenic porosity in forming initial pathways for groundwater flow. The Honey Creek HSU is considered water bearing and is likely the most transmissive part of the Glen Rose Limestone based on field observations and water-level data from the Camp Stanley area (fig. 1). Many large springs issue from this HSU within the study area including Honey Creek Spring, which supplies base flow to the Guadalupe River (fig. 1). The Honey Creek cave system is the longest known cave system in Texas; more than 20 miles of the cave system have been mapped (Smith and Veni, 1994; Texas State Historical Association, 2016).

Hensell Hydrostratigraphic Unit (Kheh)

The Hensell HSU (fig. 3) is 0–61 ft thick in the study area and is the uppermost HSU of the Pearsall Formation. The upper part of the Hensell HSU contains fabric-selective interparticle and moldic porosity; the lower part of the Hensell HSU contains fabric-selective moldic and shelter porosity (Clark and others, 2014). Minor amounts of non-fabric-selective cave porosity are present in both the upper and lower parts of the Hensell HSU. The cave porosity is likely associated with roof collapse of caves in the underlying Cow Creek HSU (Clark and others, 2014). The Hensell HSU transitions from being a water-bearing unit in the study area to a confining unit in the subsurface southeast of the study area. The Hensell HSU also transmits groundwater to the Honey Creek cave system.

Cow Creek Hydrostratigraphic Unit (Kcccc)

The Cow Creek HSU (fig. 3) is approximately 40–72 ft thick in the study area. It contains fabric-selective interparticle, moldic, and burrow porosity. It also contains non-fabric-selective vug, bedding plane, fracture, channel, and cave porosity (Clark and others, 2014). In areas that contain biostromes of coral and rudist, the HSU contains well-developed interconnected moldic porosity. In addition, the strandplain parts of the Cow Creek HSU contain interconnected fabric-selective fenestral porosity (Owens and Kerans, 2010). The Cow Creek HSU is water bearing and the primary source for water-well production within the middle zone of the Trinity aquifer (TWDB, 2023). The Cow Creek HSU receives recharge through the overlying Hensell HSU (Reeves, 1967; Ashworth, 1983). The porosity and other hydrogeologic characteristics of the Cow Creek HSU facilitate groundwater/surface-water exchanges with the Guadalupe and Blanco Rivers. Periods of recharge from the Guadalupe and Blanco Rivers to the Cow Creek HSU or of groundwater discharge from the HSU to these rivers depend on the hydrologic gradient of the groundwater flow system; relatively high groundwater levels would favor discharge from the Cow Creek HSU to the streams (Winter and others, 1999). South of the Guadalupe River, the Cow Creek HSU is more likely recharged laterally by fault juxtaposition with the Glen Rose Limestone (Veni, 1994) and possibly recharged vertically along fractures through the Glen Rose Limestone.

Hammett Hydrostratigraphic Unit (Khah)

The Hammett HSU (fig. 3) is approximately 50 ft thick in the study area. It is not exposed at the surface in the study area; however, because of the stratigraphic thicknesses of the overlying units, it is shown on the hydrostratigraphic map (fig. 2) where it is inferred to underlie areas along the Guadalupe River. On the basis of field observations and reported data (Ashworth, 1983; Wierman and others, 2010; Clark and others, 2014), the Hammett HSU functions as a confining unit, restricting the downward migration of groundwater and resulting in the formation of springs near the base of the Cow Creek HSU.

Hydrologic Characteristics of Structure

Groundwater recharge and flow paths in the study area are influenced not only by the hydrostratigraphic characteristics of the individual HSUs but also by faults and fractures. As stated in Clark and others (2013), faulting associated with the Balcones fault zone (1) might affect groundwater flow paths by forming a barrier to flow that forces groundwater to flow parallel to the fault plane (Maclay, 1995), (2) might affect groundwater flow paths by increasing flow across the fault because of fracturing and juxtaposing porous and permeable units, or (3) might have no effect on the groundwater flow paths. On the basis of the work of Small (1986), Maclay (1995) stated that faults could be barriers to groundwater flow paths where the aquifer is offset by 50 percent or more, causing groundwater to flow parallel to the fault. Clark and Journey (2006, p. 2) noted that “the amount of displacement along a particular fault tends to vary, and thus the effectiveness of a fault as a barrier to flow probably changes along the fault plane. Near a fault tip (that is, where a fault ends) no barrier to flow exists; as displacement down the fault plane increases, the effectiveness of the fault as a barrier to flow increases.” Faulting and the resulting structures (grabens and horsts) common in fault zones like the Balcones fault zone may increase the potential of controlling or altering local groundwater flow (Pantea and others, 2014) by juxtaposing permeable and less

permeable lithologies against one another. Dye-tracing studies by Johnson and others (2010) indicate that the permeable zones in juxtaposed members might be narrow; however, if cavernous permeability is present, then all available water might be transmitted at or through the fault. When juxtaposed against zones with relatively more permeability, zones with relatively less permeability might function as a barrier to groundwater flow (Stein and Ozuna, 1995).

According to Ferrill and Morris (2003), faults within the Edwards Group are more dilatant (open) than in the Glen Rose Limestone because the Edwards Group lithologies are more competent. They also stated that fault deformation increases permeability at or near faults. Fault permeability in the Glen Rose Limestone is heterogeneous and affects groundwater flow both parallel and perpendicular to faults (Ferrill and Morris, 2003). Faulting processes in the Glen Rose Limestone are complex and affect groundwater flow. Cross-fault groundwater flow is likely inhibited by clay and shale smears along fault planes and by calcite deposition in the faults and fractures (Ferrill and Morris, 2003). Solutionally enlarged fractures and conduits might also form parallel to the dip of relay ramps in the Edwards Group (Clark and Journey, 2006) because of the northeast to southwest extension.

According to Veni (1988), cave formation is strongly guided by secondary fractures that form because of faulting, rather than by the actual fault plane. Clark and Journey (2006) stated that the fractures in the study area generally are either parallel to, or perpendicular to, the main fault trend of the Balcones fault zone. Faulting affects cave development through fractures that form because of extension perpendicular to the Balcones fault zone (Clark and Journey, 2006). As extension of the series of en echelon, northwest to southeast faults associated with the Balcones fault zone occurred, the same amount of material had to occupy a larger area, resulting in extension perpendicular to the fault zone (Clark and Journey, 2006).

From field observations and previous studies, it is apparent that the hydrologic connection between the Edwards and Trinity aquifers and between the various HSUs is complex. The complexity of the aquifer system results from a combination of the original depositional history, bioturbation, primary and secondary porosity, diagenesis, and fracturing of the area from faulting. All of these factors have resulted in development of modified porosity, permeability, and transmissivity within and between the aquifers. The original depositional sediments have produced layers of shales, impure limestones, and limestones which in turn have varying types of porosity related to biological activity and to subsequent diagenesis. Faulting produced highly fractured areas that have allowed for rapid infiltration of water and subsequently formed solutionally enhanced fractures, bedding planes, channels, and caves that are highly permeable and transmissive. The juxtaposition of the individual HSUs from faulting has resulted in areas of interconnectedness between the Edwards and Trinity aquifers and the various HSUs that form the aquifers.

Summary

During 2020–22, the U.S. Geological Survey, in cooperation with the Edwards Aquifer Authority, refined the results of a previous assessment of the geologic framework and hydrostratigraphy of the Edwards and Trinity aquifers that was completed during 2014–16 within northern Bexar and Comal Counties, Texas. The Edwards and Trinity aquifers are primary sources of water for agriculture, industry, and urban and rural communities in south-central Texas. To help water-resource managers, drinking-water suppliers, and policymakers effectively manage the water resources in the area, refined maps and descriptions of the geologic framework and hydrostratigraphic units (HSUs) of the aquifers in northern Bexar and Comal Counties were developed. Groundwater flow and storage in the Edwards and Trinity aquifers are largely controlled by the geologic framework and hydrostratigraphy of the aquifers and by faulting and fractures; therefore, a refined characterization of these hydrogeologic features will be useful to water-resource managers who need to anticipate and mitigate issues related to changing land use and increasing groundwater demands.

This report presents an updated description of the geologic framework and hydrostratigraphy of the Edwards and Trinity aquifers within northern Bexar and Comal Counties. The report includes a detailed 1:24,000-scale hydrostratigraphic map, names, and descriptions of the geology and HSUs in the study area. The mapped HSUs are intended to aid in identifying units that likely facilitate groundwater recharge or discharge or function as a confining layer.

The scope of the report is focused on the geologic framework of the geologic units that contain the Edwards and Trinity aquifers and the hydrostratigraphy of the Edwards and Trinity aquifers within northern Bexar and Comal Counties. Descriptions of parts of the adjacent upper confining unit to the Edwards aquifer and lower confining unit to the middle zone of the Trinity aquifer are included in the report.

The study area covers approximately 866 square miles of northern Bexar County and Comal County, Tex. The upgradient part of the study area includes outcrops of the rocks that contain the Edwards and Trinity aquifers, and the downgradient part of the study area includes outcrops of the overlying confining units (Washita, Eagle Ford, Austin, and Taylor Groups). The rocks within the study area are sedimentary and range in age from Early to Late Cretaceous. The Miocene-age Balcones fault zone is the primary structural feature within the study area. The fault zone is an extensional system of faults that generally trends southwest to northeast in south-central Texas. The faults have normal throw, are en echelon, and are mostly downthrown to the southeast.

Two informal geologic units not identified in previous U.S. Geological Survey reports were identified in this study, and their corresponding informal HSU names are introduced in this report: a burrowed member (Seco Pass HSU [Kkb]) of the Kainer Formation of the Edwards Group and a patch reef

unit (Herff Falls HSU [Kgrhf]) of the lower member of the Glen Rose Limestone of the Trinity Group. These two informal units were identified through the continued understanding and expansion of the study area. As greater thicknesses of the newly identified HSUs were observed in the new areas of study, it became evident that these units had been seen before, in the previously mapped areas, but their footprint was minimal in those areas and therefore not recognized.

The Trinity Group rocks were deposited during the Early Cretaceous on a large, shallow marine carbonate platform (Comanche shelf) as clastic-carbonate "couplets" during three marine transgressional events that caused the sea level to rise and shoreline to move inland. These three distinct "couplets" deposited sediments that formed (1) the Hosston and Sligo Formations; (2) the Hammett Shale Member and the Cow Creek Limestone Member of the Pearsall Formation; and (3) the Hensell Sand Member of the Pearsall Formation, as well as the lower and upper members of the Glen Rose Limestone.

The Early Cretaceous Edwards Group rocks were deposited in an open marine to supratidal flats environment during two marine transgressions. The rocks that compose the Edwards Group were deposited on the landward margin of the Comanche shelf, which was sheltered from storm waves and deep ocean currents by the Stuart City reef trend in the ancestral Gulf of Mexico. Following tectonic uplift, subaerial exposure, and erosion near the end of Early Cretaceous time, the area of present-day south-central Texas was again submerged during the Late Cretaceous by a marine transgression resulting in deposition of the Georgetown Formation of the Washita Group. Much of the Georgetown Formation was subsequently removed during a marine regressive cycle. The Stuart City reef was breached, resulting in deposition of the Del Rio Clay of the Washita Group. This transgressive episode continued through the deposition of the Buda Limestone of the Washita Group, Eagle Ford Group, Austin Group, and Taylor Group.

The Trinity Group contains shale, mudstone to grainstone, boundstone, sandstone, and argillaceous limestone and is composed of the Hosston, Sligo, and Pearsall Formations and the Glen Rose Limestone. The Pearsall Formation is further subdivided into the Hammett Shale, Cow Creek Limestone, and Hensell Sand Members. The Glen Rose Limestone is subdivided into the lower and upper members.

The Edwards Group, which overlies the Trinity Group, is composed of mudstone to grainstone, dolomitic mudstone, and chert. In the study area, the Edwards Group is composed of the Kainer and Person Formations. The Kainer Formation is subdivided into (bottom to top) the basal nodular, burrowed, dolomitic, Kirschberg Evaporite, and grainstone members. The Person Formation is subdivided into (bottom to top) the regional dense, leached and collapsed (undivided), and cyclic and marine (undivided) members.

The principal structural feature in northern Bexar and Comal Counties is the Balcones fault zone, which is the result of Miocene-age faulting and fracturing. The primary orientation of mapped fractures and faults in the study area is southwest to northeast between 45 and 50 degrees. The conjugant fractures trend perpendicular to the Balcones fault zone at approximately 145–150 degrees.

Hydrostratigraphically the rocks exposed in the study area represent a section of the upper confining unit to the Edwards aquifer, the Edwards aquifer, the upper zone of the Trinity aquifer, the middle zone of the Trinity aquifer, and the lower confining unit to the middle zone of the Trinity aquifer. In the study area the Edwards aquifer is contained in the Georgetown Formation and in the rocks forming the Edwards Group. The Trinity aquifer is contained in the rocks forming the Trinity Group. The Edwards and Trinity aquifers are karstic with secondary permeability and porosity associated with bedding planes, fractures, and caves.

The Taylor Group (Pecan Gap Chalk [Kpg]), Austin Group (Ka), Eagle Ford Group (Kef), Buda Limestone (Kb), and Del Rio Clay (Kdr) collectively are generally considered to be the upper confining unit to the Edwards aquifer and do not supply appreciable amounts of water to wells in the study area.

The Edwards aquifer was subdivided into HSUs I to VIII. A ninth informal HSU (Seco Pass HSU) was added on the basis of additional field observations made by the authors in counties adjoining the study area. The Georgetown Formation of the Washita Group contains HSU I (Kg). The Person Formation of the Edwards Group contains HSUs II (cyclic and marine members, undivided [Kpcm]), III (leached and collapsed members, undivided [Kplc]), and IV (regional dense member [Kprd]), and the Kainer Formation of the Edwards Group contains HSUs V (grainstone member [Kkg]), VI (Kirschberg Evaporite Member [Kkke]), VII (dolomitic member [Kkd]), Seco Pass (burrowed member [Kkb], where present), and VIII (basal nodular member [Kkbn]).

The Trinity aquifer was subdivided into upper, middle, and lower aquifer units (hereinafter referred to as "zones"). The upper zone of the Trinity aquifer is contained in the upper member of the Glen Rose Limestone. The middle zone of the Trinity aquifer is contained in the lower member of the Glen Rose Limestone, Hensell Sand, and Cow Creek Limestone. The regionally extensive Hammett Shale forms a confining unit between the middle and lower zones of the Trinity aquifer. The lower zone of the Trinity aquifer consists of the Hosston and Sligo Formations, which do not crop out in the study area.

The upper zone of the Trinity aquifer is subdivided into five informal HSUs (top to bottom): cavernous (Kgrc), Camp Bullis (Kgrcb), upper evaporite (Kgrue), fossiliferous (Kgrf; upper [Kgruf] and lower [Kgrlf] subunits), and lower evaporite (Kgrle). The HSUs within the middle zone of the Trinity aquifer are (top to bottom) the Bulverde (Kgrb), Little Blanco (Kgrlb), Twin Sisters (Kgrts), Doeppenschmidt (Kgrd), Herff Falls (Kgrhf, where present), Rust (Kgrr), Honey Creek (Kgrhc), Hensell (Kheh), and Cow Creek (Kcccc) HSUs. Because the Herff Falls HSU is formed within a series of patch reefs that trend along a specific zone through the study area, it is not present in all locations and is equivalent in age to the Little Blanco, Twin Sisters, and Doeppenschmidt HSUs. The

underlying Hammett (Khah) HSU is a regional confining unit between the middle and lower zones of the Trinity aquifer. The lower zone of the Trinity aquifer is not exposed in the study area.

Groundwater recharge and flow paths in the study area are influenced not only by the hydrostratigraphic characteristics of the individual HSUs but also by faults and fractures. Faulting associated with the Balcones fault zone (1) might affect groundwater flow paths by forming a barrier to flow which results in water moving parallel to the fault plane, (2) might affect groundwater flow paths by increasing flow across the fault because of fracturing and juxtaposing porous and permeable units, or (3) might have no effect on the groundwater flow paths.

The effects of faulting on cave development may be from fracture development that forms from extension perpendicular to the Balcones fault zone. As extension of the series of en echelon, northwest to southeast faults associated with the Balcones fault zone occurred, the same amount of material had to occupy a larger area, resulting in extension perpendicular to the fault zone. Solutionally enlarged fractures and conduits may form parallel to the dip of relay ramps in the Edwards Group because of the northeast to southwest extension.

The hydrologic connection between the Edwards and Trinity aquifers and the various HSUs is complex. The complexity of the aquifer system results from a combination of the original depositional history, bioturbation, primary and secondary porosity, diagenesis, and fracturing of the area from faulting. All of these factors have resulted in development of modified porosity, permeability, and transmissivity within and between the aquifers. Faulting produced highly fractured areas that have allowed for rapid infiltration of water and subsequently formed solutionally enhanced fractures, bedding planes, channels, and caves that are highly permeable and transmissive. The juxtaposition of the individual HSUs from faulting has resulted in areas of interconnectedness between the Edwards and Trinity aquifers and the various HSUs that form the aquifers.

References Cited

Adkins, W.C., 1932, The Mesozoic System in Texas, *in* Sellards, E.H., Adkins, W.C., and Plummer, F.B., eds., The geology of Texas: Austin, Tex., University of Texas, Publication 3252, p. 329–518, accessed December 8, 2022, at https://store.beg.utexas.edu/ut-bulletins/167-bk3232.html.

Amsbury, D.L., 1974, Stratigraphic petrology of lower and middle Trinity rocks on the San Marcos platform, south-central Texas, *in* Aspects of Trinity geology, v. 8 *of* Geoscience and man: Baton Rouge, La., Louisiana State University, School of Geoscience, p. 1–35, accessed August 22, 2023, at https://catalog.princeton.edu/catalog/9916194553506421.

Arnow, T., 1959, Ground-water geology of Bexar County, Texas: Texas Board of Water Engineers Bulletin 5911, 62 p., accessed December 8, 2022, at https://www.twdb.texas.gov/publications/reports/bulletins/doc/Bull.htm/B5911.asp.

Arnow, T., 1963, Ground-water geology of Bexar County, Texas: U.S. Geological Survey Water-Supply Paper 1588, 36 p., 12 pls., accessed December 7, 2022, at https://doi.org/10.3133/wsp1588.

Ashworth, J.B., 1983, Ground-water availability of the Lower Cretaceous formations in the Hill Country of south-central Texas: Texas Department of Water Resources Report 273, 172 p., accessed August 22, 2023, at https://www.edwardsaquifer.org/wp-content/uploads/2019/02/1983_Ashworth_GroundWaterAvailability.pdf.

Ashworth, J.B., Stein, W.G., Donnelly, A.C.A., Persky, K., and Jones, J.P., 2001, The lower Trinity aquifer of Bandera and Kerr Counties, Texas: Plateau Regional Water Planning Group and Texas Water Development Board, prepared by LBG-Guyton and Associates and Jones Geological Consulting, 128 p., accessed December 6, 2022, at http://www.twdb.texas.gov/publications/reports/contracted_reports/doc/0704830695_RegionJ/Reference_LowerTrinity.pdf.

Banta, J.R., and Clark, A.K., 2012, Groundwater levels and water-quality observations pertaining to the Austin Group, Bexar County, Texas, 2009–11: U.S. Geological Survey Scientific Investigations Report 2012–5278, 18 p., 2 app., accessed December 7, 2022, at https://doi.org/10.3133/sir20125278.

Barker, R.A., and Ardis, A.F., 1996, Hydrogeological framework of the Edwards-Trinity aquifer system, west-central Texas: U.S. Geological Survey Professional Paper 1421–B, 61 p., accessed December 6, 2022, at https://doi.org/10.3133/pp1421B.

Barker, R.A., Bush, P.W., and Baker, E.T., 1994, Geologic history and hydrogeologic setting of the Edwards-Trinity aquifer system, west-central Texas: U.S. Geological Survey Water-Resources Investigations Report 94–4039, 38 p., accessed May 6, 2022, at https://doi.org/10.3133/wri944039.

Barnes, V.E., and Shell Development Co., Amerada Petroleum Corp., Brown, T.E., Waechter, N.B., and Dillon, R.L., 1982, Geologic atlas of Texas, San Antonio sheet—Robert Hamilton Cuyler memorial edition *in* Geologic atlas of Texas (rev. 1982): Austin, Tex., University of Texas, Bureau of Economic Geology, 1 sheet, scale 1:250,000, accessed December 6, 2022, at https://ngmdb.usgs.gov/Prodesc/proddesc_19384.htm.

Bates, R.L., and Jackson, J.A., eds., 1987, Glossary of geology (3d ed.): Alexandria, Va., American Geological Institute, 788 p., accessed December 5, 2022, at https://doi.org/10.3133/pp1421B.

Blome, C.D., and Clark, A.K., 2014, Key subsurface data help to refine Trinity aquifer hydrostratigraphic units, south-central Texas: U.S. Geological Survey Data Series 768, 1 sheet, accessed May 6, 2022, at https://doi.org/10.3133/ds768.

Blome, C.D., Faith, J.R., Pedraza, D.E., Ozuna, G.B., Cole, J.C., Clark, A.K., Small, T.A., and Morris, R.R., 2005, Geologic map of the Edwards aquifer recharge zone, south-central Texas: U.S. Geological Survey Scientific Investigations Map 2873, 1 sheet, scale 1:200,000, accessed December 3, 2022, at https://doi.org/10.3133/sim2873.

Choquette, P.W., and Pray, L.C., 1970, Geologic nomenclature and classification of porosity in sedimentary carbonates: American Association of Petroleum Geologists Bulletin, v. 54, no. 2, p. 207–250, accessed December 6, 2022, at https://archives.datapages.com/data/bulletns/1968-70/data/pg/0054/0002/0200/0207.htm.

Clark, A.K., 2003, Geologic framework and hydrogeologic features of the Glen Rose Limestone, Camp Bullis Training Site, Bexar County, Texas: U.S. Geological Survey Water Resources Investigations Report 03–4081, 9 p., 1 pl., scale 1:24,000, accessed August 22, 2023, at https://doi.org/10.3133/wri034081.

Clark, A.K., 2004, Geologic framework and hydrogeologic characteristics of the Glen Rose Limestone, Camp Stanley Storage Activity, Bexar County, Texas: U.S. Geological Survey Scientific Investigations Map 2831, 1 sheet, scale 1:24,000, accessed August 22, 2023, at https://doi.org/10.3133/sim2831.

Clark, A.K., Blome, C.D., and Morris, R.R., 2014, Geology and hydrostratigraphy of Guadalupe River State Park and Honey Creek State Natural Area, Kendall and Comal Counties, Texas: U.S. Geological Survey Scientific Investigations Map 3303, 1 sheet, scale 1:24,000, 8-p. pamphlet, accessed May 6, 2022, at https://doi.org/10.3133/sim3303.

Clark, A.K., Faith, J.R., Blome, C.D., and Pedraza, D.E., 2006, Geologic map of the Edwards aquifer in northern Medina and northeastern Uvalde Counties, south-central Texas: U.S. Geological Survey Open-File Report 2006–1372, 23 p., 1 pl., scale 1:75,000, accessed July 20, 2018, at https://doi.org/10.3133/ofr20061372.

Clark, A.K., Golab, J.A., and Morris, R.R., 2016a, Geologic framework, hydrostratigraphy, and ichnology of the Blanco, Payton, and Rough Hollow 7.5-minute quadrangles, Blanco, Comal, Hays, and Kendall Counties, Texas: U.S. Geological Survey Scientific Investigations Map 3363, 1 sheet, scale 1:24,000, 21-p. pamphlet, accessed March 30, 2023, at https://doi.org/10.3133/sim3363.

Clark, A.K., Golab, J.A., and Morris, R.R., 2016b, Geologic framework and hydrostratigraphy of the Edwards and Trinity aquifers within northern Bexar and Comal Counties, Texas: U.S. Geological Survey Scientific Investigations Map 3366, 1 sheet, scale 1:24,000, 28-p. pamphlet, accessed March 30, 2023, at https://doi.org/10.3133/sim3366.

Clark, A.K., and Journey, C.A., 2006, Flow paths in the Edwards aquifer, northern Medina and northeastern Uvalde Counties, Texas, based on hydrologic identification and geochemical characterization and simulation: U.S. Geological Survey Scientific Investigations Report 2006–5200, 48 p., accessed December 6, 2022, at https://doi.org/10.3133/sir20065200.

Clark, A.K., and Morris, R.R., 2015, Geologic and hydrostratigraphic map of the Anhalt, Fischer, and Spring Branch 7.5-minute quadrangles, Blanco, Comal, and Kendall Counties, Texas: U.S. Geological Survey Scientific Investigations Map 3333, 1 sheet, scale 1:50,000, 13-p. pamphlet, accessed November 15, 2022, at https://doi.org/10.3133/sim3333.

Clark, A.K., Pedraza, D.E., and Morris, R.R., 2013, Geologic framework, structure, and hydrogeologic characteristics of the Knippa Gap area in eastern Uvalde and western Medina Counties, Texas: U.S. Geological Survey Scientific Investigations Report 2013–5149, 35 p., 1 pl., accessed May 6, 2022, at https://doi.org/10.3133/sir20135149.

Clark, A.R., Blome, C.D., and Faith, J.R., 2009, Map showing the geology and hydrostratigraphy of the Edwards aquifer catchment area, northern Bexar County, south-central Texas: U.S. Geological Survey Open-File Report 2009–1008, 24 p., 1 pl., scale 1:50,000, accessed July 20, 2018, at https://doi.org/10.3133/ofr20091008.

Collins, E.W., 1991, Geologic map of the Hunter 7.5-minute quadrangle, Comal and Hays Counties: U.S. Geological Survey open-file map prepared by University of Texas at Austin, Bureau of Economic Geology, under cooperative agreement, 1 sheet, scale 1:24,000, accessed December 7, 2022, at https://store.beg.utexas.edu/statemap-project-maps/1745-ofm0099.html.

Collins, E.W., 1992a, Geologic map of the Anhalt 7.5-minute quadrangle, Comal County, Texas: U.S. Geological Survey open-file map prepared by University of Texas at Austin, Bureau of Economic Geology, under cooperative agreement 14-08-0001-A0885, 1 sheet, scale 1:24,000, accessed December 7, 2022, at https://store.beg.utexas.edu/statemap-project-maps/2420-ofm0095.html.

Collins, E.W., 1992b, Geologic map of the Fischer 7.5-minute quadrangle, Comal and Blanco Counties, Texas: U.S. Geological Survey open-file map prepared by University of Texas at Austin, Bureau of Economic Geology, under cooperative agreement 14-08-0001-A0885, 1 sheet, scale 1:24,000, accessed December 7, 2022, at https://store.beg.utexas.edu/statemap-project-maps/905-ofm0030.html.

Collins, E.W., 1992c, Geologic map of the Smithson Valley 7.5-minute quadrangle, Comal County, Texas: U.S. Geological Survey open-file map prepared by University of Texas at Austin, Bureau of Economic Geology, under cooperative agreement 14-08-0001-A0885, 1 sheet, scale 1:24,000, accessed December 7, 2022, at https://store.beg.utexas.edu/statemap-project-maps/2409-ofm0106.html.

Collins, E.W., 1993a, Geologic map of the New Braunfels East 7.5-minute quadrangle, Comal and Guadalupe Counties, Texas: U.S. Geological Survey open-file map prepared by University of Texas at Austin, Bureau of Economic Geology, under cooperative agreement 14334-92-A-1085, 1 sheet, scale 1:24,000, accessed December 7, 2022, at https://store.beg.utexas.edu/statemap-project-maps/2511-ofm0024.html.

Collins, E.W., 1993b, Geologic map of the New Braunfels West 7.5-minute quadrangle, Comal and Guadalupe Counties, Texas: U.S. Geological Survey open-file map prepared by University of Texas at Austin, Bureau of Economic Geology, under cooperative agreement 14334-92-A-1085, 1 sheet, scale 1:24,000, accessed December 7, 2022, at https://store.beg.utexas.edu/statemap-project-maps/1534-ofm0023.html.

Collins, E.W., 1993c, Geologic map of the Schertz 7.5-minute quadrangle, Bexar, Comal, and Guadalupe Counties, Texas: U.S. Geological Survey open-file map prepared by University of Texas at Austin, Bureau of Economic Geology, under cooperative agreement 14334-92-A-1085, 1 sheet, scale 1:24,000, accessed December 7, 2022, at https://store.beg.utexas.edu/statemap-project-maps/2479-ofm0015.html.

Collins, E.W., 1993d, Geologic map of the Bat Cave 7.5-minute quadrangle, Comal County, Texas: U.S. Geological Survey open-file map prepared by University of Texas at Austin, Bureau of Economic Geology, under cooperative agreement 14334-92-A-1085, 1 sheet, scale 1:24,000, accessed December 7, 2022, at https://store.beg.utexas.edu/statemap-project-maps/2418-ofm0097.html.

Collins, E.W., 1993e, Geologic map of the Bulverde 7.5-minute quadrangle, Bexar and Comal Counties, Texas: U.S. Geological Survey open-file map prepared by University of Texas at Austin, Bureau of Economic Geology, under cooperative agreement 14334-92-A-1085, 1 sheet, scale 1:24,000, accessed December 8, 2022, at https://store.beg.utexas.edu/statemap-project-maps/2513-ofm0022.html.

Collins, E.W., 1994a, Geologic map of the Longhorn quadrangle, Texas: U.S. Geological Survey open-file map prepared by University of Texas at Austin, Bureau of Economic Geology, under cooperative agreement 1434-93-A-1174, 1 sheet, scale 1:24,000, accessed December 8, 2022, at https://store.beg.utexas.edu/statemap-project-maps/2480-ofm0016.html.

Collins, E.W., 1994b, Geologic map of the Camp Bullis quadrangle, Texas: U.S. Geological Survey open-file map prepared by University of Texas at Austin, Bureau of Economic Geology, under cooperative agreement 1434-93-A-1174, 1 sheet, scale 1:24,000, accessed December 8, 2022, at https://store.beg.utexas.edu/statemap-project-maps/2514-ofm0021.html.

Collins, E.W., 1994c, Geologic map of the Castle Hills quadrangle, Texas: U.S. Geological Survey open-file map prepared by University of Texas at Austin, Bureau of Economic Geology, under cooperative agreement 1434-93-A-1174, 1 sheet, scale 1:24,000, accessed December 8, 2022, at https://store.beg.utexas.edu/statemap-project-maps/2481-ofm0017.html.

Collins, E.W., 1994d, Geologic map of the Bergheim quadrangle, Texas: U.S. Geological Survey open-file map prepared by University of Texas at Austin, Bureau of Economic Geology, under cooperative agreement 1434-93-A-1174, 1 sheet, scale 1:24,000, accessed December 8, 2022, at https://store.beg.utexas.edu/statemap-project-maps/2510-ofm0025.html.

Collins, E.W., 1995a, Geologic map of the San Geronimo quadrangle, Texas: U.S. Geological Survey open-file map prepared by University of Texas at Austin, Bureau of Economic Geology, under cooperative agreement 1434-94-A-1255, 1 sheet, scale 1:24,000, accessed December 8, 2022, at https://store.beg.utexas.edu/statemap-project-maps/2483-ofm0019.html.

Collins, E.W., 1995b, Geologic map of the Van Raub quadrangle, Texas: U.S. Geological Survey open-file map prepared by University of Texas at Austin, Bureau of Economic Geology, under cooperative agreement 1434-94-A-1255, 1 sheet, scale 1:24,000, accessed December 8, 2022, at https://store.beg.utexas.edu/statemap-project-maps/2484-ofm0020.html.

Collins, E.W., 1995c, Geologic map of the Helotes quadrangle, Texas: U.S. Geological Survey open-file map prepared by University of Texas at Austin, Bureau of Economic Geology, under cooperative agreement 1434-94-A-1255, 1 sheet, scale 1:24,000, accessed December 8, 2022, at https://store.beg.utexas.edu/statemap-project-maps/2482-ofm0018.html.

Collins, E.W., 1995d, Geologic map of the Jack Mountain quadrangle, Texas: U.S. Geological Survey open-file map prepared by University of Texas at Austin, Bureau of Economic Geology, under cooperative agreement 1434-94-A-1255, 1 sheet, scale 1:24,000, accessed December 8, 2022, at https://store.beg.utexas.edu/statemap-project-maps/2415-ofm0100.html.

Collins, E.W., 2000, Geologic map of the New Braunfels, Texas, 30 x 60 minute quadrangle—Geologic framework of an urban-growth corridor along the Edwards aquifer, south-central Texas: Austin, Tex., University of Texas, Bureau of Economic Geology, Miscellaneous Map no. 39, 28 p., scale 1:100,000, accessed December 8, 2022, at https://store.beg.utexas.edu/statemap-project-maps/2511-ofm0024.html.

Collins, E.W., Baumgardner, R.W., Jr., and Raney, J.A., 1991, Geologic map of the Sattler 7.5-minute quadrangle, Comal County, Texas: U.S. Geological Survey open-file map prepared by University of Texas at Austin, Bureau of Economic Geology, under cooperative agreement, 1 sheet, scale 1:24,000, accessed December 8, 2022, at https://store.beg.utexas.edu/statemap-project-maps/2410-ofm0105.html.

Collins, E.W., and Hovorka, S.D., 1997, Structure map of the San Antonio segment of the Edwards aquifer and Balcones fault zone, south-central Texas—Structural framework of a major limestone aquifer—Kinney, Uvalde, Medina, Bexar, Comal, and Hays Counties: Austin, Tex., University of Texas, Bureau of Economic Geology, Miscellaneous Map no. 38, 2 sheets, scale 1:250,000, accessed December 8, 2022, at https://www.edwardsaquifer.org/wp-content/uploads/2019/02/1997_CollinsHovorka_StructureMap.pdf.

Curry, W.H., 1934, Fredericksburg-Washita (Edwards-Georgetown) contact in Edwards Plateau region of Texas—Geological notes: American Association of Petroleum Geologist Bulletin, December 1, 1934, v. 18, p. 1698–1705, accessed August 21, 2023, at https://doi.org/10.1306/3D932C9C-16B1-11D7-8645000102C1865D.

Denne, R.A., Breyer, J.A., Callender, A.D., Hinote, R.E., Kariminia, M., Kosanke, T.H., Kita, Z., Lees, J.A., Rowe, H., Spaw, J.M., and Tur, N., 2016, Biostratigraphic and geochemical constraints on the stratigraphy and depositional environments of the Eagle Ford and Woodbine Groups of Texas, *in* Breyer, J.A., ed., The Eagle Ford Shale—A renaissance in U.S. oil production: American Association of Petroleum Geologists Memoir 110, p. 1–86, accessed August 22, 2023, at https://pubs.geoscienceworld.org/aapg/books/book/1514/chapter/107189403/Biostratigraphic-and-Geochemical-Constraints-on.

Douglass, R.C., 1960, The foraminiferal genus *Orbitolina* in North America: U.S. Geological Survey Professional Paper 333, 52 p., accessed July 25, 2018, at https://doi.org/10.3133/pp333.

Droser, M.J., and Bottjer, D.J., 1986, A semiquantitative field classification of ichnofabric: Journal of Sedimentary Research, v. 56, no. 4, p. 558–559, accessed December 8, 2022, at https://pubs.geoscienceworld.org/sepm/jsedres/article-abstract/56/4/558/113776/A-semiquantitative-field-classification-of.

Dunham, R.J., 1962, Classification of carbonate rocks according to depositional texture, *in* Classification of Carbonate Rocks Symposium: American Association of Petroleum Geologists Memoir 1, p. 108–121, accessed December 8, 2022, at https://pubs.geoscienceworld.org/aapg/books/book/1475/chapter/107178011/Classification-of-Carbonate-Rocks-According-to.

Ehrenberg, K., 1944, Ergänzende Bemerkungen zu den seinerzeit aus dem Miozän von Burgschleinitz beschriebenen Gangkernen und Bauten dekapoder Krebse: Palaontologische Zeitschrift, v. 23, nos. 3–4, p. 354–359, accessed August 22, 2023, at https://link.springer.com/article/10.1007/BF03160443.

Esri, 2016, ArcGIS desktop—Release 10: Redlands, Calif., Esri software release, accessed August 22, 2023, at https://www.esri.com/en-us/home.

Faith, J.R., 2004, Strain and fractures in an extensional relay ramp, Sierra del Carmen, Black Gap Wildlife Management Area, Brewster County, Texas—Implications for determining structural controls on groundwater flow pathways in the Edwards aquifer, south-central Texas: San Antonio, Tex., University of Texas, master's thesis, 88 p.

Ferrill, D.A., and Morris, A.P., 2003, Dilational normal faults: Journal of Structural Geology, v. 25, no. 2, p. 183–196, accessed December 8, 2022, at https://www.sciencedirect.com/journal/journal-of-structural-geology/vol/25/issue/2.

Ferrill, D.A., Sims, D.W., Morris, A.P., Waiting, D.J., and Franklin, N.M., 2003, Structural controls on the Edwards aquifer/Trinity aquifer interface in the Camp Bullis quadrangle, Texas: Edwards Aquifer Authority and U.S. Army Corps of Engineers, prepared by CNWRA, Southwest Research Institute, San Antonio, Tex., and Department of Earth and Environmental Science, University of Texas at San Antonio, San Antonio, Tex., December 5, 2003, 126 p., accessed June 5, 2013, at https://www.edwardsaquifer.org/wp-content/uploads/2019/05/2003_Ferrill-etal_StructuralControlsCampBullisQuadrangle.pdf.

Finsley, C., 1989, A field guide to fossils of Texas—Texas Monthly field guide series: Texas Monthly Press, 189 p.

Fisher, W.L., and Rodda, P.U., 1969, Edwards Formation (Lower Cretaceous), Texas—Dolomitization in a carbonate platform system: American Association of Petroleum Geologist Bulletin, v. 55, no. 1, p. 55–72, accessed August 22, 2023, at https://pubs.geoscienceworld.org/aapgbull/article/53/1/55/103925/Edwards-Formation-Lower-Cretaceous-Texas.

Gary, M.O., Veni, G., Shade, B., and Gary, R.H., 2011, Spatial and temporal recharge variability related to groundwater interconnection of the Edwards and Trinity aquifers, Camp Bullis, Bexar and Comal Counties, Texas, *in* Interconnection of the Trinity (Glen Rose) and Edwards aquifers along the Balcones fault zone and related topics—Karst Conservation Initiative meeting, Austin, Tex., February 17, 2011, [Proceedings]: Austin, Tex., Karst Conservation Initiative, 46 p., accessed December 8, 2022, at https://digitalcommons.usf.edu/cgi/viewcontent.cgi?article=1070&context=kip_talks.

Garza, S., 1962, Recharge, discharge, and changes in ground water storage in the Edwards and associated limestones, San Antonio area, Texas—A progress report of studies, 1955–59: Texas Water Development Board Bulletin 6201, 42 p., accessed July 25, 2018, at https://www.twdb.texas.gov/publications/reports/bulletins/doc/B6201.pdf.

George, P.G., Mace, R.E., and Petrossian, R., 2011, Aquifers of Texas: Texas Water Development Board Report 380, 172 p., accessed December 8, 2022, at https://www.twdb.texas.gov/publications/reports/numbered_reports/index.asp.

George, W.O., 1952, Geology and ground-water resources of Comal County, Texas, *with sections on* Surface-water runoff, by S.D. Breeding, and Chemical character of the water, by W.W. Hastings: U.S. Geological Survey Water Supply Paper 1138, 126 p., 3 pls., accessed July 25, 2018, at https://doi.org/10.3133/wsp1138.

Golab, J.A., Smith, J.J., Clark, A.K., and Morris, R.R., 2017, Bioturbation-influenced fluid pathways within a carbonate platform system—The Lower Cretaceous (Aptian–Albian) Glen Rose Limestone: Palaeogeography, Palaeoclimatology, Palaeoecology, v. 465, p. 138–155, accessed August 21, 2023, at https://www.sciencedirect.com/science/article/pii/S0031018216306319?via%3Dihub.

Hanson, J.A., and Small, T.A., 1995, Geologic framework and hydrogeologic characteristics of the Edwards aquifer outcrop, Hays County, Texas: U.S. Geological Survey Water-Resources Investigations Report 95–4265, 10 p., accessed December 6, 2022, at https://doi.org/10.3133/wri954265.

Hantzschel, W., 1962, Trace fossils and problematica, *in* Moore, R.C., ed., Treatise on invertebrate paleontology—Part W, miscellanea: Geological Society of America and University of Kansas Press, p. W177–W245.

Hatch, S.L., Umphres, K.C., and Ardoin, A.J., 2016, Field guide to common Texas grasses: Texas A&M AgriLife Research and Service Series, 448 p.

Hill, R.T., 1891, The Comanche Series of the Texas-Arkansas region: Geological Society of America Bulletin, v. 2, no. 1, p. 503–528, accessed January 5, 2022, at https://doi.org/10.1130/GSAB-2-503.

Hill, R.T., 1892, Geologic evolution of the non-mountainous topography of the Texas region—An introduction to the study of the Great Plains: American Geologist, v. 10, no. 2, p. 105–115, accessed December 8, 2022, at https://babel.hathitrust.org/cgi/pt?id=mdp.39015068249930&view=1up&seq=129.

Hill, R.T., 1900, Topographic atlas of the United States, folio 3—Physical geography of the Texas region: Washington, D.C., U.S. Geological Survey, 26 p., accessed December 8, 2022, at https://repositories.lib.utexas.edu/handle/2152/78006.

Hill, R.T., 1901, Geography and geology of the Black and Grand Prairies, Texas, with detailed descriptions of the Cretaceous formations and special reference to artesian waters, *in* Walcott, C.D., ed., Twenty-first annual report of the United States Geological Survey to the Secretary of the Interior, 1899–1900—Part VII, Texas: U.S. Geological Survey Annual Report 21, p. 128–337, accessed December 7, 2022, at https://doi.org/10.3133/ar21_7.

Hovorka, S.D., Dutton, A.R., Ruppel, S.C., and Yeh, J.S., 1996, Edwards aquifer ground-water resources—Geologic controls on porosity development in platform carbonates, south Texas: Austin, Tex., University of Texas, Bureau of Economic Geology Report of Investigations no. 238, 75 p., accessed December 7, 2022, at https://store.beg.utexas.edu/reports-of-investigations/1201-ri0238.html.

Hus, R., Acocella, V., Funiciello, R., and De Batist, M., 2005, Sandbox models of relay ramp structure and evolution: Journal of Structural Geology, v. 27, no. 3, p. 459–473, accessed December 7, 2022, at https://www.sciencedirect.com/science/article/pii/S0191814104002019.

Imlay, R.W., 1940, Lower Cretaceous and Jurassic formations of southern Arkansas and their oil and gas possibilities: Arkansas Geological Survey Information Circular, no. 12, 64 p., accessed December 8, 2022, at https://www.geology.arkansas.gov/docs/pdf/publication/information-circulars/IC-12.pdf.

Imlay, R.W., 1945, Subsurface Lower Cretaceous formations of south Texas: American Association of Petroleum Geologists Bulletin, v. 29, no. 10, p. 1416–1469, accessed December 7, 2022, at https://pubs.geoscienceworld.org/aapgbull/article/29/10/1416/546990/Subsurface-Lower-Cretaceous-Formations-of-South.

Inden, R.F., 1974, Lithofacies and depositional model for a Trinity Cretaceous sequence, central Texas, *in* Aspects of Trinity geology, v. 8 *of* Geoscience and man: Baton Rouge, La., Louisiana State University, School of Geoscience, p. 37–52, accessed January 9, 2023, at https://catalog.princeton.edu/catalog/9916194553506421.

Johnson, S., Esquilin, R., Mahula, D., Thompson, E., Mireles, J., Gloyd, R., Sterzenback, J., Hoyt, J., and Schindel, G., 2002, Hydrogeologic data report for 2001: Edwards Aquifer Authority Report 02–01, p. 1–3, accessed December 7, 2022, at https://www.edwardsaquifer.org/wp-content/uploads/2019/05/2002_Johnson-etal_2001HydrogeologicData.pdf.

Johnson, S., Schindel, G., and Veni, G., 2010, Tracing groundwater flow paths in the Edwards aquifer recharge zone, Panther Springs Creek Basin, northern Bexar County, Texas (May 2010): Edwards Aquifer Authority Report 10–01, 112 p., accessed August 22, 2023, at https://www.edwardsaquifer.org/wp-content/uploads/2019/02/2010_Johnson-etal_PantherSpringsFlowpaths.pdf.

Klappa, C.F., 1980, Rhizoliths in terrestrial carbonates—Classification, recognition, genesis and significance: Sedimentology, v. 27, no. 6, p. 613–629, accessed December 4, 2022, at https://onlinelibrary.wiley.com/doi/pdf/10.1111/j.1365-3091.1980.tb01651.x.

Kuniansky, E.L., and Ardis, A.F., 2004, Hydrogeology and ground-water flow in the Edwards-Trinity aquifer system, west-central Texas—Regional aquifer-system analysis—Edwards-Trinity: U.S. Geological Survey Professional Paper 1421–C, 78 p., accessed August, 21, 2023, at https://doi.org/10.3133/pp1421C.

Land, L.F., and Dorsey, M.E., 1988, Reassessment of the Georgetown Limestone as a hydrogeologic unit of the Edwards aquifer, Georgetown area, Texas: U.S. Geological Survey Water-Resources Investigations Report 88–4090, 54 p., accessed December 4, 2022, at https://doi.org/10.3133/wri884190.

Loucks, R.G., and Kerans, C., 2003, Lower Cretaceous Glen Rose "Patch Reef" Reservoir in the Chittim Field, Maverick County, South Texas: Gulf Coast Association of Geological Societies Transactions, v. 53, p. 490–503, accessed December 4, 2022, at https://archives.datapages.com/data/gcags/data/053/053001/pdfs/0490.pdf.

Lozo, F.E., and Stricklin, F.L., Jr., 1956, Stratigraphic notes on the outcrop basal Cretaceous, central Texas: Gulf Coast Association of Geological Societies Transactions, v. 6, p. 67–78, accessed December 4, 2022, at https://archives.datapages.com/data/gcags/data/006/006001/pdfs/0067.pdf.

Maclay, R.W., 1995, Geology and hydrology of the Edwards aquifer in the San Antonio area, Texas: U.S. Geological Survey Water-Resources Investigations Report 95–4186, 69 p., accessed December 4, 2022, at https://doi.org/10.3133/wri954186.

Maclay, R.W., and Small, T.A., 1976, Progress report on geology of the Edwards aquifer, San Antonio area, Texas, and preliminary interpretation of borehole geophysical and laboratory data on carbonate rocks: U.S. Geological Survey Open-File Report 76–627, 65 p., accessed August 22, 2023, at https://doi.org/10.3133/ofr76627.

Maclay, R.W., and Small, T.A., 1983, Hydrostratigraphic subdivisions and fault barriers of the Edwards aquifer, south-central Texas: Journal of Hydrology, v. 61, no. 1–3, p. 127–146, accessed December 4, 2022, at https://www.sciencedirect.com/science/article/pii/0022169483902391.

Maclay, R.W., and Small, T.A., 1986, Carbonate geology and hydrology of the Edwards aquifer in the San Antonio area, Texas: Texas Water Development Board, Report 296, 90 p., accessed November 15, 2022, at https://www.twdb.texas.gov/publications/reports/numbered_reports/index.asp.

Martin, K.G., 1967, Stratigraphy of the Buda Limestone, south-central Texas: Society of Economic Paleontologists and Mineralogists, Permian Basin Section, Publication no. 67–8, p. 286–299, accessed December 4, 2022, at https://utsa.primo.exlibrisgroup.com/discovery/search?vid=01UTXSANT_INST:DEFAULT&query=any,contains,00930647.

Martinez, N., 1982, A regional subsurface study of the Austin Chalk, south Texas: Waco, Tex., Baylor University, master's thesis, 113 p., accessed December 4, 2022, at https://baylor.primo.exlibrisgroup.com/discovery/fulldisplay?docid=alma991013400879705576&context=L&vid=01BUL_INST:BAYLOR&lang=en&search_scope=MyInst_and_CI&adaptor=Local%20Search%20Engine&tab=Everything&query=any,contains,A%20regional%20subsurface%20study%20of%20the%20Austin%20Chalk,%20south%20Texas,AND&mode=advanced&offset=0.

Murray, G., 1961, Geology of the Atlantic and Gulf Coastal Province of North America: New York, Harper, 692 p.

Ockerman, D.J., 2007, Simulation of streamflow and estimation of ground-water recharge in the upper Cibolo Creek watershed, south-central Texas, 1992–2004: U.S. Geological Survey Scientific Investigations Report 2007–5202, 34 p., accessed May 6, 2022, at https://doi.org/10.3133/sir20075202.

Owens, L., and Kerans, C., 2010, Revisiting the Cow Creek Limestone—Facies architecture and depositional history of a greenhouse strandplain: Gulf Coast Association of Geological Societies Transactions, v. 60, p. 907–915, accessed March 8, 2023, at https://archives.datapages.com/data/gcags_pdf/2010/Papers/owenkera.htm.

Pantea, M.P., Blome, C.D., and Clark, A.K., 2014, Three-dimensional model of the hydrostratigraphy and structure of the area in and around the U.S. Army–Camp Stanley Storage Activity Area, northern Bexar County, Texas: U.S. Geological Survey Scientific Investigations Report 2014–5074, 13 p., accessed May 6, 2022, at https://doi.org/10.3133/sir20145074.

Pedraza, D.E., Clark, A.K., Golab, J.A., and Morris, R.R., 2023, Geospatial dataset for the geologic framework and hydrostratigraphy of the Edwards and Trinity aquifers within northern Bexar and Comal Counties, Texas, at 1:24,000: U.S. Geological Survey data release, https://doi.org/10.5066/P9GXJ2RS.

Pemberton, S.G., and Frey, R.W., 1982, Trace fossil nomenclature and the Planolites-Paleophycus dilemma: Journal of Paleontology, v. 56, no. 4, p. 843–881, accessed December 8, 2022, at https://pubs.geoscienceworld.org/jpaleontol/article/56/4/843/108052/Trace-fossil-nomenclature-and-the-Planolites.

Perkins, B.F., 1974, Paleoecology of a rudist reef complex in the Comanche Cretaceous Glen Rose Limestone of central Texas, *in* Aspects of Trinity geology, v. 8 *of* Geoscience and man: Baton Rouge, La., Louisiana State University, School of Geoscience, p. 131–173, accessed August 22, 2023, at https://catalog.princeton.edu/catalog/9916194553506421.

Petitt, B.M., Jr., and George, W.O., 1956, Ground-water resources of the San Antonio area, Texas—A progress report of current studies: Texas Board of Water Engineers Bulletin 5608, v. 1, 80 p., accessed December 8, 2022, at https://www.twdb.texas.gov/publications/reports/bulletins/doc/B5608_V1.pdf.

Petta, T.J., 1977, Abstract—Diagenesis and geochemistry of a Glen Rose patch reef complex, Bandera County, Texas: Gulf Coast Association of Geological Societies Transactions, v. 27, p. 442–443, accessed December 8, 2022, at https://archives.datapages.com/data/gcags/data/027/027001/0442b.htm.

Puente, C., 1978, Method of estimating natural recharge to the Edwards aquifer in the San Antonio area, Texas: U.S. Geological Survey Water-Resources Investigations Report 78–10, 34 p., accessed December 8, 2022, at https://doi.org/10.3133/wri7810.

Raney, J.A., and Collins, E.W., 1991, Geologic map of the Devils Backbone 7.5-minute quadrangle, Comal and Hays Counties: U.S. Geological Survey open-file map prepared by University of Texas at Austin, Bureau of Economic Geology, under cooperative agreement, 1 sheet, scale 1:24,000, accessed December 8, 2022, at https://store.beg.utexas.edu/statemap-project-maps/1537-ofm0031.html.

Reeves, R.D., 1967, Ground-water resources of Kendall County, Texas: Texas Water Development Board Report 60, 101 p., accessed November 15, 2022, at https://www.twdb.texas.gov/publications/reports/numbered_reports/doc/R60/R60.pdf.

Richardson, G.B., 1904, Report of a reconnaissance in Trans-Pecos Texas north of the Texas and Pacific Railway: University of Texas, Mineral Survey Bulletin, no. 9, 119 p., accessed August 22, 2023, at https://repositories.lib.utexas.edu/handle/2152/24408.

Roemer, F., 1852, Die Kreidebildungen von Texas und ihre organischen Einschlüsse [The Cretaceous formations of Texas and their organic inclusions]: Bonn, Germany, Adolph Marcus Publishing, 100 p., 11 pls., [In German], accessed December 8, 2022, at https://www.biodiversitylibrary.org/item/51697#page/5/mode/1up.

Rose, P.R., 1972, Edwards Group, surface and subsurface, central Texas: Austin, Tex., University of Texas, Bureau of Economic Geology Report of Investigations 74, 198 p., accessed December 8, 2022, at https://doi.org/10.23867/RI0074D.

Ryan, M., and Meiman, J., 1996, An examination of short-term variations in water quality at a karst spring in Kentucky: Ground Water, v. 34, no. 1, p. 23–30, accessed December 8, 2022, at https://doi.org/10.1111/j.1745-6584.1996.tb01861.x.

Scott, R.W., Molineux, A.M., and Mancini, E.A., 2007, Lower Albian sequence stratigraphy and coral buildups—Glen Rose Formation, Texas, USA, *in* Scott, R.W., ed., Cretaceous rudists and carbonate platforms—Environmental feedback: Society for Sedimentary Publication no. 87, p. 181–191, accessed December 8, 2022, at https://doi.org/10.2110/pec.07.87.

Seilacher, A., 2007, Trace fossil analysis: Berlin, Springer-Verlag, 226 p.

Sellards, E.H., Adkins, W.S., and Plummer, F.B., 1932, The geology of Texas, volume 1—Stratigraphy: Austin, Tex., University of Texas, Bulletin 3232, scale 1:2,000,000, accessed December 8, 2022, at https://repositories.lib.utexas.edu/handle/2152/60618.

Small, T.A., 1986, Hydrogeologic sections of the Edwards aquifer and its confining units in the San Antonio area, Texas: U.S. Geological Survey Water-Resources Investigations Report 85–4259, 52 p., accessed December 8, 2022, at https://doi.org/10.3133/wri854259.

Small, T.A., and Hanson, J.A., 1994, Geologic framework and hydrogeologic characteristics of the Edwards aquifer outcrop, Comal County, Texas: U.S. Geological Survey Water-Resources Investigations Report 94–4117, 10 p., accessed December 8, 2022, at https://doi.org/10.3133/wri944117.

Smith, A.R., and Veni, G., 1994, Karst regions of Texas, *in* Elliott, W., and Veni, G., eds., The caves and karst of Texas—National Speleological Society, 1994 Convention, Brackettville, Tex., June 19–24, 1994, Guidebook: Huntsville, Ala., National Speleological Society, p. 7–12.

Smith, B.D., Cain, M.J., Clark, A.K., Moore, D.W., Faith, J.R., and Hill, P.L., 2005, Helicopter electromagnetic and magnetic survey data and maps, northern Bexar County, Texas: U.S. Geological Survey Open-File Report 2005–1158, 122 p., accessed December 8, 2022, at https://doi.org/10.3133/ofr20051158.

Stein, W.G., and Ozuna, G.B., 1995, Geologic framework and hydrogeologic characteristics of the Edwards aquifer recharge zone, Bexar County, Texas: U.S. Geological Survey Water-Resources Investigations Report 95–4030, 8 p., accessed December 8, 2022, at https://doi.org/10.3133/wri954030.

Stricklin, F.L., Jr., and Smith, C.I., 1973, Environmental reconstruction of a carbonate beach complex, Cow Creek (Lower Cretaceous) Formation of central Texas: Geological Society of America Bulletin, v. 84, no. 4, p. 1349–1368, accessed December 8, 2022, at https://pubs.geoscienceworld.org/gsa/gsabulletin/article/84/4/1349/201374/Environmental-Reconstruction-of-a-Carbonate-Beach.

Stricklin, F.L., Jr., Smith, C.I., and Lozo, F.E., 1971, Stratigraphy of Lower Cretaceous Trinity deposits of central Texas: Austin, Tex., University of Texas, Bureau of Economic Geology Report of Investigations 71, 63 p., accessed December 8, 2022, at https://store.beg.utexas.edu/reports-of-investigations/1819-ri0071.html.

Texas State Historical Association, 2016, Handbook of Texas online—Caves: Texas State Historical Association web page, accessed June 28, 2016, at https://tshaonline.org/handbook/online/articles/rqc03.

Texas Water Development Board [TWDB], 2023, Water Data Interactive Groundwater Data Viewer: Texas Water Development Board website, accessed February 22, 2023, at https://www3.twdb.texas.gov/apps/WaterDataInteractive/GroundwaterDataViewer/?map=gwdb.

Trevino, R.H., 1988, Facies and depositional environments of the Boquillas Formation, upper Cretaceous of southwest Texas: Arlington, Tex., University of Texas, master's thesis, p. 54–63, accessed January 5, 2023, at https://uta.alma.exlibrisgroup.com/discovery/openurl?institution=01UTAR_INST&rfr_id=info:sid%2Fsummon&rft_dat=ie%3D51103687450004911,language%3DEN&svc_dat=CTO&u.ignore_date_coverage=true&vid=01UTAR_INST:Services.

Trudgill, B.D., 2002, Structural controls on drainage development in the Canyonlands grabens of southeast Utah, USA, *in* Underhill, J.R., and Trudgill, B.D., eds., The structure and stratigraphy of rift systems: American Association of Petroleum Geologists Bulletin Special Issue, v. 86, no. 6, p. 1095–1112, accessed December 6, 2022, at https://www.researchgate.net/publication/279604140_Structural_controls_on_drainage_development_in_the_Canyonlands_Grabens_of_Southeast_Utah.

U.S. Census Bureau, 2022, Fastest-growing cities are still in the west and south: U.S. Census Bureau web page, accessed August 22, 2023, at https://www.census.gov/newsroom/press-releases/2022/fastest-growing-cities-population-estimates.html#:~:text=Eight%20of%20the%2015%20fastest-growing%20large%20cities%20or,in%20the%20South%20and%20four%20in%20the%20West.

U.S. Geological Survey, 2022a, Karst aquifers—What is karst?: U.S. Geological Survey Water Resources Mission Area web page, accessed December 6, 2022, at https://water.usgs.gov/ogw/karst/pages/whatiskarst.

U.S. Geological Survey, 2022b, National Geologic Map Database—Geolex search: U.S. Geological Survey database, accessed December 6, 2022, at http://ngmdb.usgs.gov/Geolex/search.

Veni, G., 1988, The caves of Bexar County (2d ed.): Austin, Tex., Texas Memorial Museum, University of Texas, Speleological Monographs, v. 2, 300 p., accessed December 6, 2022, at https://www.texasspeleologicalsurvey.org/PDF/TNSC_Pubs/Veni-Bexar-PublicR.pdf.

Veni, G., 1994, Geomorphology, hydrology, geochemistry, and evolution of the karstic Lower Glen Rose aquifer, south-central Texas: Pennsylvania State University, Ph.D. dissertation, 712 p., accessed December 8, 2022, at https://www.texasspeleologicalsurvey.org/publications/TSS_Monographs.php.

Veni, G., 2005, Lithology as a predictive tool of conduit morphology and hydrology in environmental impact assessments, *in* Multidisciplinary Conference on Sinkholes and the Engineering and Environmental Impacts of Karst (10th), San Antonio, Tex., September 24–28, 2005 [Proceedings]: American Society of Civil Engineers, p. 46–56, accessed December 8, 2022, at https://ascelibrary.org/doi/abs/10.1061/40796%28177%296.

Veni, G., 2021, National Cave and Karst Research Institute field guide 1—A cross section of central Texas cave and karst management—Show caves, preserves, and private property: Carlsbad, N. Mex., National Cave and Karst Research Institute, 36 p., accessed December 9, 2022, at https://nckri.org/wp-content/uploads/2021/10/NCKRI-FG-1.pdf.

Weeks, A.W., 1945, Balcones, Luling, and Mexia fault zones in Texas: American Association of Petroleum Geologists Bulletin, v. 29, p. 1733–1737, accessed December 8, 2022, at https://pubs.geoscienceworld.org/aapgbull/article/29/12/1733/547004/Balcones-Luling-and-Mexia-Fault-Zones-in-Texas1.

Wells, J.W., 1932, Corals of the Trinity Group of the Comanchean of central Texas: Journal of Paleontology, v. 6, no. 3, p. 225–256, accessed December 8, 2022, at https://www.jstor.org/stable/1298104.

Wentworth, C.K., 1922, A scale of grade and class terms for clastic sediments: Journal of Geology, v. 30, no. 5, p. 377–392, accessed August 22, 2023, at https://www.journals.uchicago.edu/doi/epdf/10.1086/622910.

Whitney, M.I., 1952, Some zone marker fossils of the Glen Rose Formation of central Texas: Journal of Paleontology, v. 26, no. 1, p. 65–73, accessed December 8, 2022, at https://scholarly.cmich.edu/?a=d&d=CMUFac1952-02.

Wierman, D.A., Broun, A.S., and Hunt, B.B., 2010, Hydrogeologic atlas of the Hill Country Trinity aquifer, Blanco, Hays, and Travis Counties, central Texas: Hays-Trinity, Barton Springs/Edwards Aquifer, and Blanco-Pedernales Groundwater Conservation Districts, July 2010, 17 p., accessed December 8, 2022, at https://repositories.lib.utexas.edu/handle/2152/8977.

Williams, G.O., Breeding, S.D., and Hastings, W.W., 1952, Geology and ground-water resources of Comal County, Texas: U.S. Geological Survey Water-Supply Paper 1138, p. 58–59, accessed May 6, 2022, at https://doi.org/10.3133/wsp1138.

Winter, T.C., Harvey, J.W., Franke, O.L., and Alley, W.M., 1999, Groundwater and surface water—A single resource: U.S. Geological Survey Circular 1139, 88 p., accessed March 21, 2023, at https://doi.org/10.3133/cir1139.

For more information about this publication, contact
Director, Oklahoma-Texas Water Science Center
U.S. Geological Survey
1505 Ferguson Lane
Austin, TX 78754–4501

For additional information, visit
https://www.usgs.gov/centers/ot-water

Publishing support provided by
Lafayette Publishing Service Center

USGS

Clark and others—**Geologic Framework and Hydrostratigraphy of the Edwards and Trinity Aquifers, Northern Bexar and Comal Counties, Texas**—SIM 3510

ISSN 2329-132X (online)
https://doi.org/10.3133/sim3510
Supersedes USGS Scientific Investigations Map 3366